THE 105 cm SCHMIDT TELESCOPE AT THE KISO STATION OF THE TOKYO ASTRONOMICAL OBSERVATORY

By

Bunshiro TAKASE, Keiichi ISHIDA, Minoru SHIMIZU, Hideo MAEHARA,
Kiyotoshi HAMAJIMA, Takeshi NOGUCHI, and Mitsuru OHASHI

Reprinted from the
Annals of the Tokyo Astronomical Observatory
Second Series, Volume XVI, Number 2

THE 105 cm SCHMIDT TELESCOPE AT THE KISO STATION OF THE TOKYO ASTRONOMICAL OBSERVATORY

By

Bunshiro TAKASE, Keiichi ISHIDA, Minoru SHIMIZU, Hideo MAEHARA, Kiyotoshi HAMAJIMA, Takeshi NOGUCHI, and Mitsuru OHASHI

(Received Jan. 19, 1977)

Abstract

Two years have passed since the 105 cm Schmidt telescope was installed at the Kiso Station of the Tokyo Astronomical Observatory in October, 1974. During this period, adjustments, examinations, and preliminary observations have been carried out, of which process and result together with a description of main characteristics of the telescope are presented here.

Keywords: Instruments, Schmidt telescope.

1. The Kiso Station

The Kiso Station is located at the western part of Nagano Prefecture, about 200 km west of Tokyo and about 100 km north east of Nagoya (Fig. 1). The coordinates of the center of the Schmidt telescope dome have been determined referring to the Japanese geodetic datum as $-137°37'42''.2$ in longitude, $+35°47'38''.7$ in latitude, and 1,130 m in elevation above mean sea level.

It was dedicated on October 1st, 1974, as the fifth branch station of the Tokyo Observatory. The area of the site is about 6 ha, and includes three buildings. One of them is the dome of the Schmidt telescope, and the others are the house for night airglow observations and the main building which contains offices, laboratories, a library, a dining room, and sleeping rooms for observers.

2. The Telescope Building

The building containing the telescope consists of a cylindrical portion with the concrete and stone wall, and a rotating metal dome. The diameter and height of the building are 16.2 m and 19.3 m, respectively. Accessories are an outer corridor with a parapet and a staircase leading to the visitors' gallery.

The rotating dome has a slit, 4 m in width and 15.7 m in length. It is covered by a double shutter and also by upper and lower two windscreens which are driven by electric motors. It takes 1 minute to open or close the shutter completely.

The dome weighing about 100 tons is supported on twenty double-wheel trucks which ride on a circular rail mounted on the concrete wall. Eight trucks of them situated under main arches are equipped with motors which drive the wheels and rotate the dome. The rotation speed is 1/4 r. p. m.

The steel frame of the dome is covered by outer and inner shells, the former of which is a welded stainless steel plate of 2 mm thickness, and the latter a jointed thin aluminium plate.

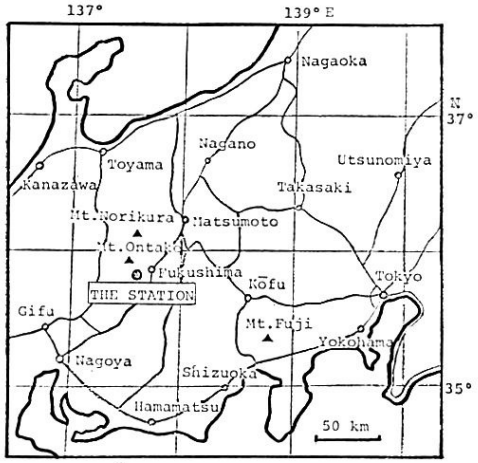

Fig. 1. *A map showing the location of the Kiso Station.*

Both shells are attached by 25 mm thick insulation boards, inside of which is covered by aluminium foil. Those structures, together with an 80 cm thick layer of the air between outer and inner shells which is ventilated by 13 motor-fans disposed along the skirt portion of the dome, have been designed to keep temperature differences in the observing room as small as possible.

The observing room is on the second floor of the building, the northern part of which is occupied by a control room, dark rooms used for loading or unloading plates, and for printing step wedge on the plates (see 7, 3) and 4)), and the eastern part by a visitors' gallery.

Above these rooms is a mezzanine floor on which an observer is easy to access to the top portion of the telescope tube in its horizontal position. This floor is used for putting on or taking off objective prisms and a hoodcap. A 1 ton crane hung from a main arch of the dome is utilized to move prisms.

Along the inner edge of the mezzanine with a U-shape opening toward south is laid a rail to rotate the truck of the observer carrier, which also goes up and down and back and forth in radial direction so that an observer can reach the eye-piece of the guide telescope at any observing position (Fig. 9 (a)).

A hole with 2 m diameter is at the western part of the observing floor, through which heavy parts of the telescope such as the main mirror are hoisted from the first floor by means of a 2.5 ton crane.

On the first floor of the building there are entrances, a resting room with a kitchenet, a switchboard and pedestal room which contains a power source unit and control circuits, and dark-rooms where pre- and post-exposure treatments of photographic plates are processed. A dumb-waiter to carry the plates connects both darkrooms on the first and the second floors.

The basement is divided into a power supply room, a workshop, a store room, and a room containing the equipment which produces the dry air to be sent into the telescope tube (See 7, 2)).

A concrete pier which is completely isolated from the building proper supports the telescope of about 70 tons.

3. Mechanical Parts of the Telescope

Highly rigid structure and smooth driving mechanisms are required for large telescopes; especially in case of large Schmidts where an indirect guiding system is used with guide

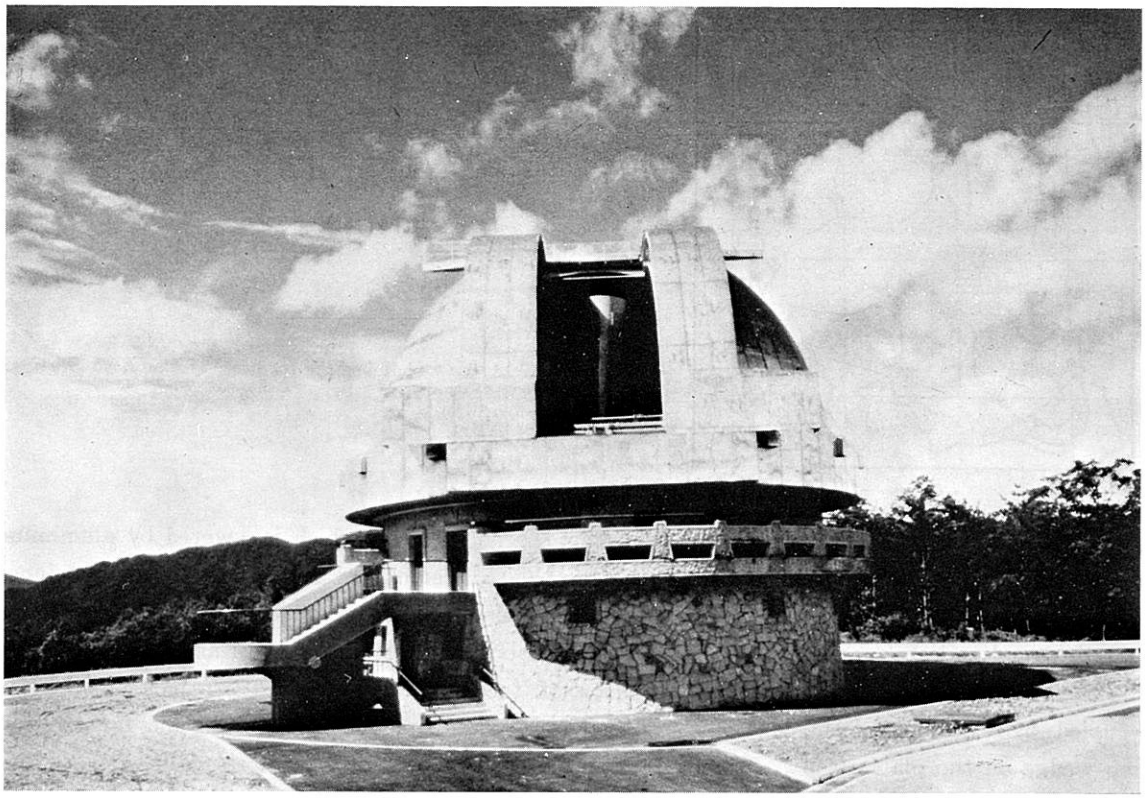

Fig. 2. *The telescope dome seen from its north-east side.*

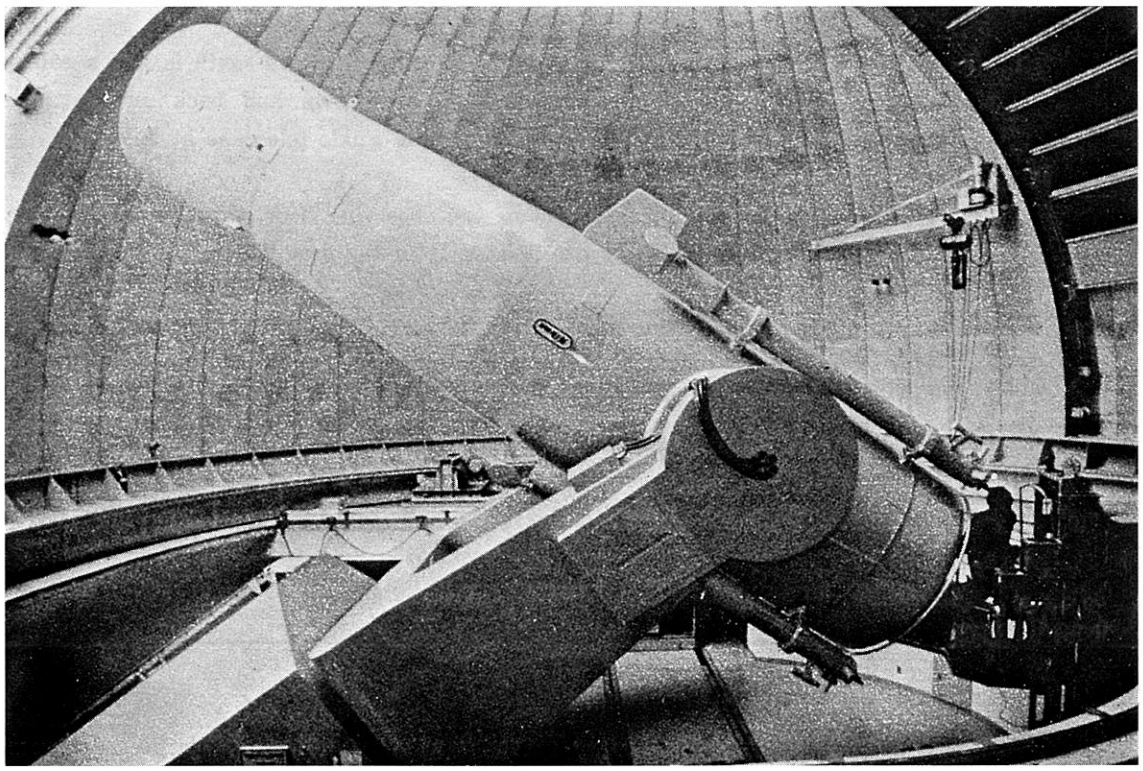

Fig. 3. *The 105 cm Schmidt telescope viewed from its east side.*

telescopes, and where the field rotation accompanied by a long exposure is a serious problem because of their large field.

1) The Mounting

The telescope has a conventional fork-type mounting. In order to avoid flexures as far as possible, the polar axis base, the fork, as well as the telescope tube and the mirror cell are all heavy constructions of welded-steel 12–15 mm thick with interior reinforcements. The weight of the telescope is in total about 70 tons, of which the polar axis including its base and the driving system occupies 34 tons, the fork and the declination axis 18 tons, and the telescope tube containing optical parts 17 tons. A concrete pier, 3.2 m×4 m and weighing 170 tons, supports the telescope.

The polar axis base is fixed on the welded-steel frame grouted on the concrete pier. Its pedestal with four legs whose lengths are individually adjustable by means of jack-screws and which have allowances of the horizontal shift is used to set the direction of the polar axis. A steel ball of 76 mm diameter which is placed under the base and directly below the center of gravity makes it easy to move the base. A push-pull screw horizontally mounted on the south side of the base helps the azimuthal setting of the axis. The direction of the axis is adjustable within ranges of ±30′ both in azimuth and altitude; the displacements are measured by the horizontal and vertical scales of 1′ graduation attached also to the south side of the base. The final setting of the polar axis was accomplished by an auto-collimation with a small mirror put on the bottom side of the polar axis, with 2″ accuracy (See 6, 2), (b)).

The polar axis is a cylinder 3550 mm long and of 900 mm diameter. It is supported by two two-row ball bearings at the upper and lower ends of the axis, the former of which is of angular-contact type carrying on the loads in both thrust and radial directions, and the latter is a radial bearing.

The fork is firmly fastened to the polar axis by means of 20 thick bolts each of which is tightened with a uniform torque. Its prongs carry the declination axis both halves of which squeeze the telescope tube through two-row angular-contact bearings. The declination axis has a diameter of 600 mm and a total span of 5 m.

Movable ranges of the polar and declination axes are ±150° in hour angle and from −49°10′ to +120°50′ (30°50′ beyond the pole) in declination respectively, at the both ends of which the telescope is stopped by means of the limit switches. Mechanical limits are also set by ±4° further than above-mentioned ranges. In addition the telescope is prohibited to go to the region where the altitude is less than 5° by an action of the mercury switch.

Deflections of the fork arms in various observing positions due to the flexure are at most 1 mm at their upper ends. However the effects of the deflection on the direction of the telescope tube appear to vary as a function of its hour angle (See 6, 2), (b)).

The torque values required to rotate the polar and declination axes when clamps are released, are 70 kg·m and 6 kg·m respectively.

2) The Driving System

There are three rates in driving speed both in right ascension and declination. Quick rate is 90°/min, slow rate 1′/sec, and fine rate has four alternatives of 1″, 2″, 4″, and 6″ per second.

The quick motion is given by a spur gear system which is driven by DC servomotor. The right ascension spur gear has 1800 mm diameter in pitch circle and 600 teeth, while the declination spur has 1200 mm diameter in pitch circle and 400 teeth. For the slow and fine motions, as well as the clock motion in right ascension a worm wheel is used which has a diameter of 2160 mm

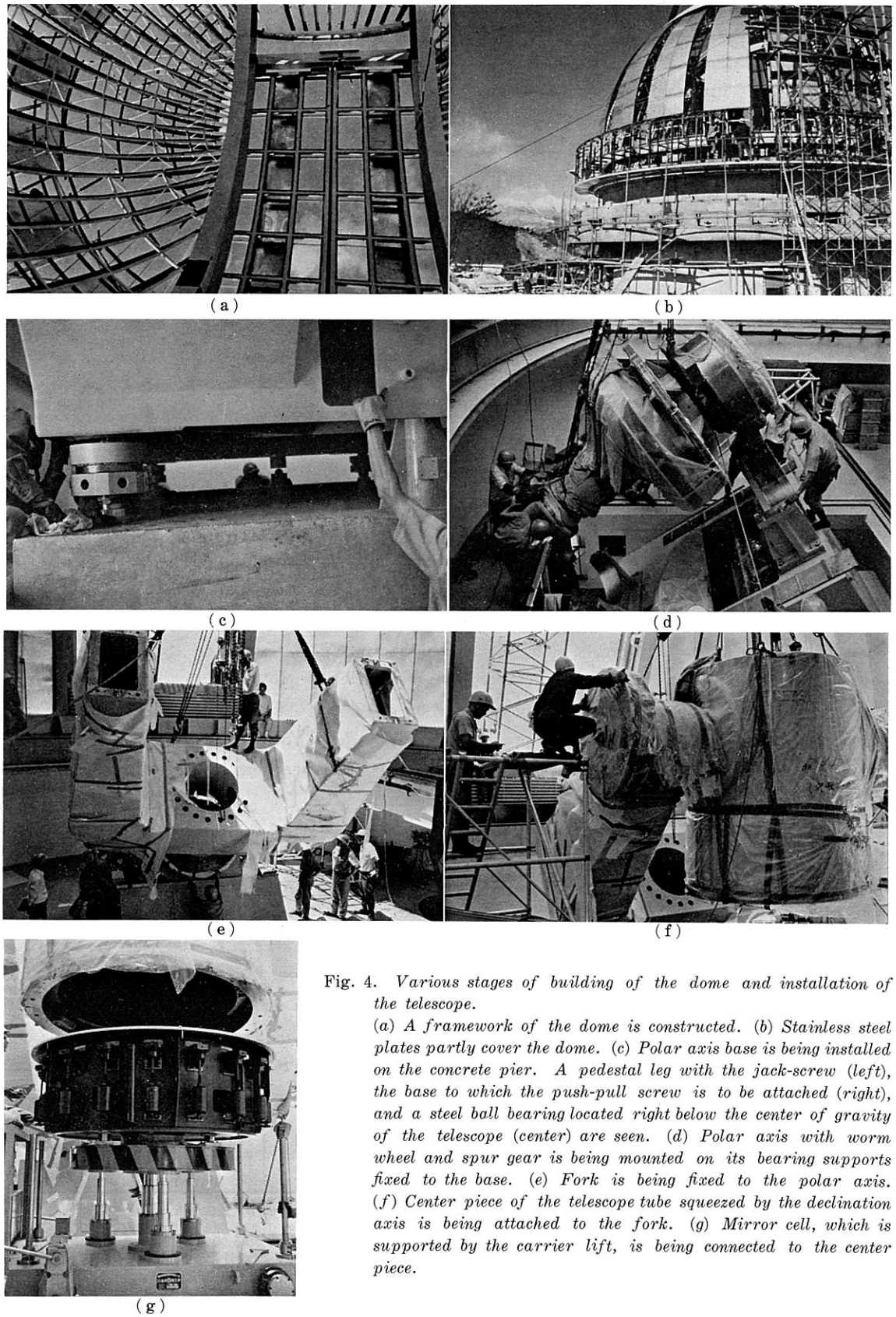

Fig. 4. *Various stages of building of the dome and installation of the telescope.*
(a) A framework of the dome is constructed. (b) Stainless steel plates partly cover the dome. (c) Polar axis base is being installed on the concrete pier. A pedestal leg with the jack-screw (left), the base to which the push-pull screw is to be attached (right), and a steel ball bearing located right below the center of gravity of the telescope (center) are seen. (d) Polar axis with worm wheel and spur gear is being mounted on its bearing supports fixed to the base. (e) Fork is being fixed to the polar axis. (f) Center piece of the telescope tube squeezed by the declination axis is being attached to the fork. (g) Mirror cell, which is supported by the carrier lift, is being connected to the center piece.

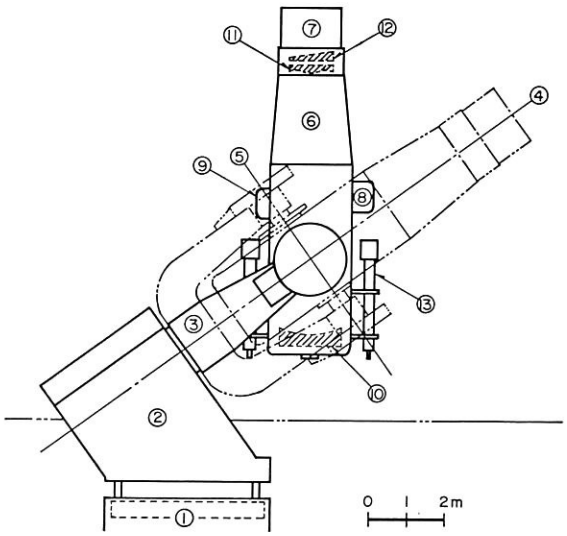

Fig. 5. *A sketch of the telescope with a scale.*
① *Base frame* ② *Polar axis base* ③ *Fork* ④ *Polar axis* ⑤ *Declination axis* ⑥ *Telescope tube* ⑦ *Hood* ⑧ *Plateholder loading box* ⑨ *Housing of filters* ⑩ *Main mirror* ⑪ *Corrector plate* ⑫ *Objective prism* ⑬ *Guide telescope*

and 720 teeth. On the other hand the slow and fine motions in declination are also provided by a worm wheel with 1200 mm diameter and 400 teeth. An AC servomotor, an AC motor, and a 60 Hz synchronous motor are used respectively for the slow, fine and clock motions. The synchronous motor is operated either by a built-in oscillator or by a commercial 60 Hz line. These motions are transmitted to the worm through the planetary gear systems (Fig. 7).

With the DC servomotor is combined a tachogenerator which applies a feedback to increase or decrease the driving speed. This feed back system makes it possible that before or after the quick rate motion, speed-up or speed-down is automatically processed.

Preloads are given to the quick spur gears by means of the torque motors to avoid the backlash of the slow gear system.

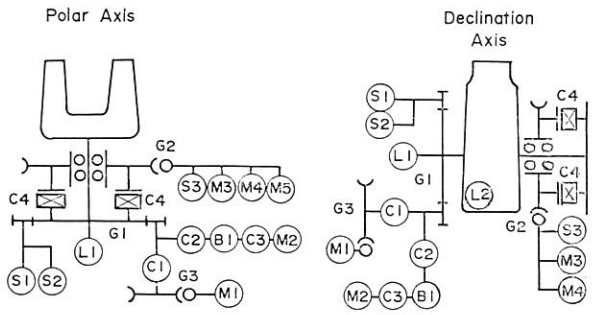

Fig. 6. *Conception chart of the gear system.*
(G1) *Spur gear* (G2) *Worm gear* (G3) *Worm gear* (C1) *Magnetic clutch* (C2) *Mechanical clutch* (C3) *Magnetic clutch* (C4) *Magnetic clutch (clamp)* (M1) *Quick motor-Tachogenerator* (M2) *Torque motor* (M3) *Fine motor* (M4) *Slow motor* (M5) *Synchronous motor* (S1) *Synchro (fine, 1′)* (S2) *Synchro (coarse, 1°)* (S3) *Incremental encoder (0″.1)* (B1) *Magnetic brake* (L1) *Limit switch* (L2) *Mercury limit switch*

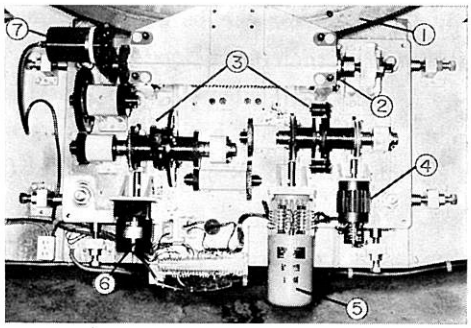

Fig. 7. *The gear train for driving the polar axis.*
① *Worm wheel* ② *Worm gear* ③ *Planetary gear system* ④ *Fine motor* ⑤ *Slow motor* ⑥ *Clock motor* ⑦ *0″.1 encoder*

Values of hour angle and declination are provided by the synchros attached to the respective spur gears, and indicated in a digital form through an A/D converter. Furthermore incremental encoders with 0.″1 division are equipped on the worm gears to make the telescope motion analysis and the computer-guide possible. Classical graduated circles of hour angle and declination, both 150 cm in diameter, are mounted on the respective axes to offer an estimation of the telescope position.

The telescope can be moved freely by hand when the electric clamp is released. This manual operation is useful for the cases when, for example, the balance of the telescope is examined and a tie-bar is connected to the telescope tube or the fork.

3) The Telescope Tube

The telescope tube consists of several portions firmly connected to one another. They are the mirror cell, the center piece, the camera section, the conical tube, the top cylinder, and the hood. The over-all length is 8.81 m and the diameter is 2.1 m at the bottom and 1.7 m at the top (Fig. 5). All portions except for the hood are made of welded-steel plate and reinforced by strong girders and ring stiffeners. The deflection of the tube in its horizontal position is 36″.

(a) The mirror cell

The mirror cell weighs 6 tons including the mirror and the lead weight pieces disposed over its bottom side. The mirror is supported by a floating mechanism consisting of 36 counter-weight levers, a half of which is for axial support and the remaining half is for radial support. The axial support is applied through pads attached to the rear side of the mirror, and the radial support through a steel belt tied round the mirror, respectively (Fig. 8).

Definition of the mirror position is accomplished in a radial direction by means of a core tube and a support tube inserted in the central hole of the mirror, while in a axial direction by three invar bars with 25 mm thickness and an expansion coefficient of 1×10^{-6}/deg. The upper ends of the three bars touch the strong ring girder to which the focus unit of the camera is tightly fixed through rigid spiders, and the lower ends are in contact with the polished surface of the metal pieces attached to the steel belt of the mirror, which is preloaded upward by three springs through counter-weight levers located just below the metal pieces. This way of the equipment of invar bars is different from that of several other Schmidt telescopes. The variation of the focal length 3300 mm is kept within ±0.05 mm for the temperature difference between $+20^\circ$ and -10°C. The tilt of the mirror can be set by adjusting the length of the invar bars with micrometer screws attached to their upper ends.

A practical device is given that the mirror can be washed without removing it from the cell. When the cell itself is detached from or attached to the center piece of the tube, a carrier with a lift operated by oil-pressure is used (Fig. 9, (b)).

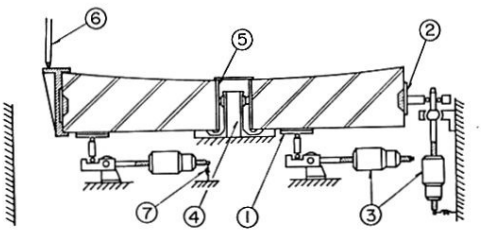

Fig. 8. *The mirror support system.*
① *Pad* ② *Steel belt* ③ *Counter-weight lever* ④ *Core tube*
⑤ *Support tube* ⑥ *Invar bar* ⑦ *Preload in axial direction*

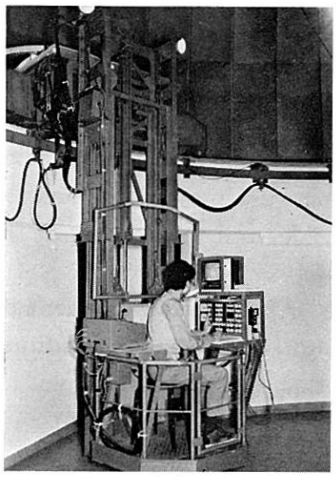

(a)

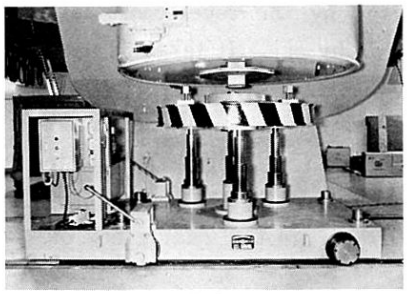

(b)

Fig. 9. *Various transporters.*
(a) The observer carrier loaded with a control system. (b) The carrier of the mirror cell equipped with a lift. (c) The car with a lift for loading the plateholder.

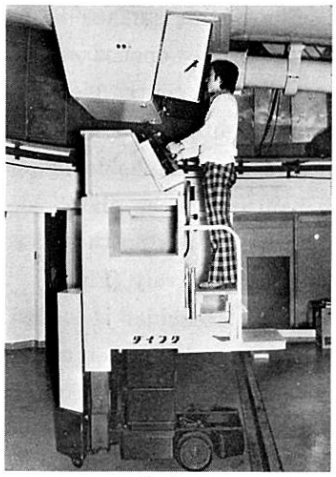

(c)

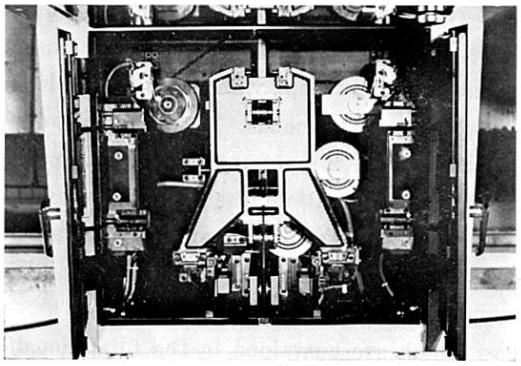

(a)

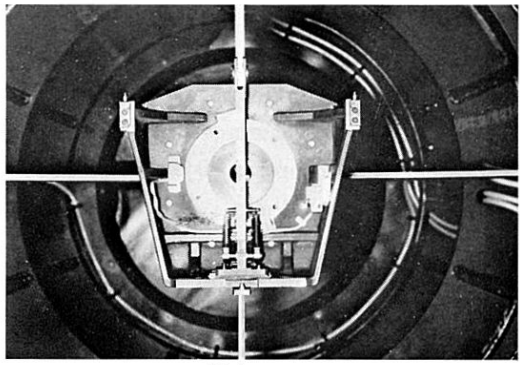

(b)

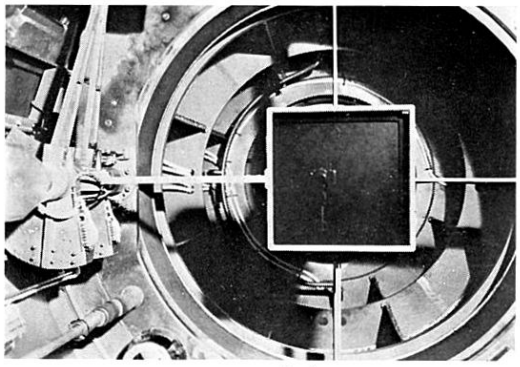

(c)

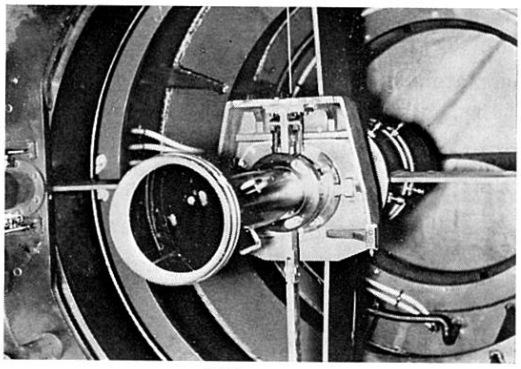

(d)

Fig. 10. *Mechanical parts inside the camera section. (a) The plateholder carriage at its terminal position in the loading box. (b) The plateholder supporter suspended by rigid spiders. (c) A plate at the exposure position in front of which the chosen filter is loaded. Filter loading mechanism is seen left side. (d) The second mirror is mounted on the plateholder supporter. (This is done in the case when Cassegrain focus is to be used.)*

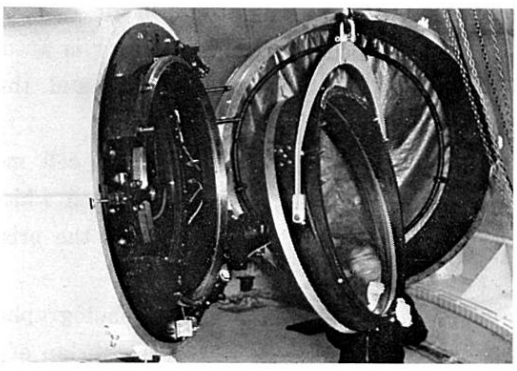

Fig. 11. (*right*) *An objective prism is being loaded after the hood is opened. The prism cell rotator attached to the top cylinder of the telescope tube is seen left side.*

The mirror surface is protected by the cover consisting of three triangular segments which are electrically opened or closed one by one. It takes 32 seconds to finish the operation.

(b) The center piece and the camera section

The center piece is the portion to which the declination axis is connected. The camera section contains the plateholder supporter which is firmly attached to the focus unit, and the loading mechanisms of the plateholder and filters (Fig. 10 (a), (b), (c)). Two outward projections from the tube seen at the north and south sides are the loading box of the holder and the housing of the filters, respectively (Fig. 5).

The plateholder is loaded or unloaded through the loading box to or from the holder carriage, the telescope being set in the so-called rest-position, where the azimuth is 180° and the altitude is about 7°. This position to load the holder is also different from that of other telescopes. A small car with electric lift is used to make the loading operation easy and safe (Fig. 9, (c)).

The carriage transports the holder to or from the supporter. The carriage-in process is that it moves upward along the rail by a tensioned wire driven by a motor, the sliding lid being left inside the loading box and the serial number of the plate being set by increasing an electromagnetic counter. The carriage-out process is the reversal of this, with the printing of the serial number on a corner of the plate by means of a flash of fluorescent numerical display and with the replacing of sliding lid. Both carriage-in and carriage-out operations take 30 seconds.

The carriage-in process is followed by the focus setting which is accomplished by an encoder in an accuracy of 0.01 mm. In case of the computer-controlled operation, the focus is automatically set to a value in accordance with a selected filter when the pointing of the telescope is instructed, while to its center value when the returning to the rest-position is commanded so that the rail can be linked properly with the plateholder supporter.

Any one of the three filters inserted in the frames which are contained in the filter housing can be selected to use. The filter loading mechanism supplies the desired filter in front of the plate by pushing the selection button on the operation panel. Filters can also be loaded inside the plateholder by hand.

The focus unit has a helicoidal gear to move the plateholder suppoter in the range of ± 25 mm. When the filter loading mechanism is employed, however, the focusing range is limited from -4 mm to $+25$ mm. In the case when the cassegrain focus is used, the secondary mirror is mounted on the plateholder supporter with an easy operation.

(c) The upper portion of the tube

To the upper end of the conical tube the top cylinder containing the cells of the corrector plate and of objective prism is connected. Right inside the corrector is located an exposure shutter of double curtain type, both parts of which move to the opposite directions. It is operated by a motor, taking 13 seconds to open or close completely. When the electricity is out a magnetic clutch is detached so that the shutter is automatically closed. The exposure is controlled by the switch button on the handset box, and the shutter can be automatically closed by setting the timer.

Outside the corrector is the prism cell mounted on its rotator (see the next section). The uppermost portion of the tube is a hood which is connected to the top cylinder with strong hinges so that it can easily be opened when the prism is loaded or unloaded.

(d) The prism cell rotator

When a crowded star field is photographed it is often desired to change the dispersion direction of the prism to minimize the overlap of the spectra as far as possible. It is also useful to

take pairs of spectra of which dispersion directions are 180° apart from each other for measuring the radial velocity of the objects.

For these purposes a rotation mechanism of the prism cell has been designed. The rotation is carried out by a rotating ring which is mounted on three sets of pair rollers. The ring has a spur gear around its periphery which is driven by a motor with a special stoppage mechanism. This motor turns the ring and can stop it with 1′ accuracy at four positions, where the vertex of the prism are precisely directed toward four cardinal points. It takes 8 minutes for the prism cell to finish a rotation.

The prism cell can also be turned round manually by pressing the free switch button located near the rotating ring. This operation is processed when the prism is loaded or unloaded.

4. The Optical Parts of the Telescope

1) The Spherical Mirror and the Corrector Plate

The main optical system of the telescope is of the classical Schmidt type and consists of the spherical mirror and the corrector plate, whose effective apertures are 1500 mm and 1050 mm, respectively. The focal length of the system is 3300 mm and the focal ratio is F/3.1 accordingly.

The spherical mirror, made of Cer-Vit C101 (manufactured by Owens-Illinois Inc., U. S. A) is 1555 mm in blank diameter and has a spherical surface with radius of curvature of 6571 mm. The thickness at the edge is 289 mm and that at the center is about 240 mm. It has a central hole with 159 mm diameter. The total weight of the mirror is 1350 kg. Its surface is aluminized.

The corrector plate, whose material is BSC 7 (manufactured by Nippon Kogaku Co. Ltd., Japan), is 1140 mm in blank diameter, 20 mm in thickness, and weighs 48 kg. The hard coating is applied to both sides. It was designed to be of type of the minimum chromatic aberration with 4358 Å as the basic wavelength. The figuring, the polishing, and the coating or aluminizing of both spherical mirror and corrector plate were processed by Nippon Kogaku.

2) Plates and Filters Used

The telescope is designed to use either 14 inch (35.6 cm) or 24 cm square glass plate, 1 mm in thickness. Various kinds of Eastman Kodak spectroscopic plate are usually employed together with several sorts of Schott color glass filters with 39 cm square size and 2 mm thickness. The usual combinations of emulsion and filter are shown in Fig. 12, which gives the sensitivity curve for each color band.

As the plate scale is 1 mm = 62″.5, the 14 inch and 24 cm square plates cover about 6° and 4° square fields, respectively. A vignetting due to the insufficient size of the spherical mirror occurs in the outer region of the plate, while that due to the occultation by the plateholder of which size is 408 mm × 408 mm arises on the whole region. The effect of the vignetting in terms of the magnitude difference between the middle portion and the corner of the plate is estimated to be 0.05 and 0.44 mag for 24 cm and 14 inch square plates, respectively. The zone of constant vignetting is within 3°.9 diameter circle.

The plate is loaded into the plateholder by a special loading apparatus so that the plate is kept bent to the curved surface with 3300 mm radius of curvature, while being exposed (see 7, 3)). Filters are loaded either by hand inside the plateholder or by the filter loader in front of the plateholder in its exposure position (see 3, 3), (b)).

3) The Cassegrain System

The Cassegrain system is also available by mounting the secondary mirror on the plateholder supporter (Fig. 10, (d)). The secondary mirror, made of the low-expansion glass, has a hyperboloidal

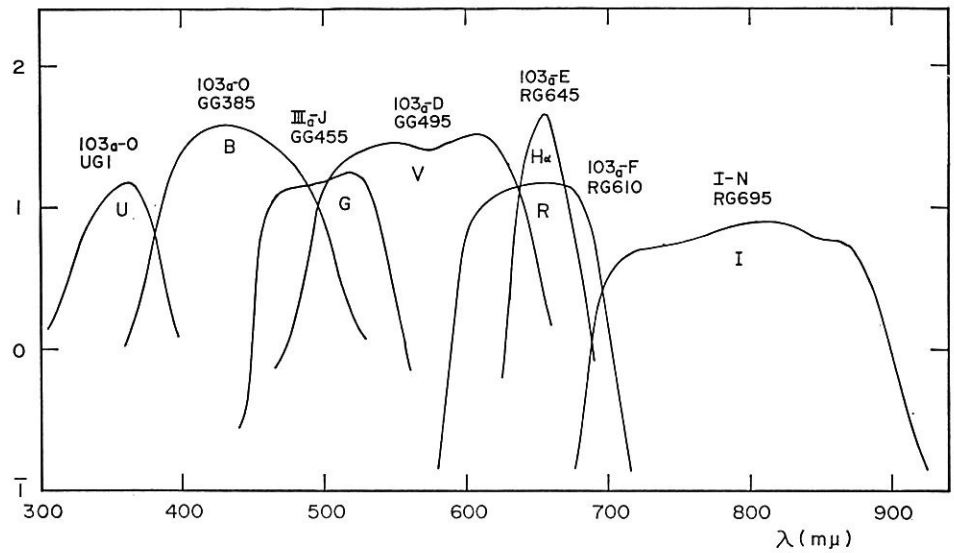

Fig. 12. *The color band system now in use, consisting of several combinations of various Eastman Kodak spectroscopic plates and Schott color glass filters. Wavelength is in abscissa and the relative sensitivity in ordinate.*

surface which is aluminized, with 175 mm effective aperture (190 mm blank diameter), 30 mm central thickness and 1.7 kg weight. When this is combined with the main mirror, the focal length of 23,760 mm and the focal ratio of 22.6 are resulted. The field range is about 10′ in diameter. It is planned to equip a photoelectric photometer at this focus.

4) Objective Prisms

Two objective prisms of which data are shown in Table 1 are now in use with the telescope. Both of them have been figured and polished by Grubb-persons & Co. Ltd., U. K.

Each prism is contained in a cell made of light alloy. Between the glass and the cell are placed small pads of delrin which is an excellent compression-resisting material. Both sides of the prisms have inclinations shown in Table 1 to the surface perpendicular to the telescope axis, the edge surface being cylindrical with the axis parallel to the telescope axis. This arrangement gives the result that the incident ray reaching the plate center is subject to the minimum deviation,

Table 1. *The Data of the Objective Prisms*

Item		No. 1	No. 2
Material		Crown glass (BK7)	Flint glass (F2)
Vertex angle		2°	4°
Inclination to the surface perpendicular to the telescope axis	upper side	0°28′	0°42′
	lower side[1]	1°32′	3°12′
Effective aperture[2]		1050 mm	1050 mm
Thickness	maximum	70 mm	108 mm
	minimum	31 mm	31 mm
Weight		121 kg	245 kg
Refractive index (for 4358Å)		1.527	1.642
Dispersion	at Hγ	800Å/mm	170Å/mm
	at A band	3800Å/mm	1000Å/mm

1) This means the side facing to the corrector plate.
2) The blank diameter of each prism is 1100 mm.

and accordingly the field correction is made minimum.

The vertex direction of the prism can be set toward each one of the four cardinal points by means of the prism rotator (See 3, 3), (d)).

5) The Guide Telescope

Two identical refractors are equipped on the telescope for guiding. They are mounted on the north-east side and south-east side of the telescope tube. The objective lens of the refractor has an aperture of 200 mm, and a focal length of 3300 mm, the latter of which is the same as that of the main telescope.

There are three eye-ends, two of which are furnished with eye-pieces for viewing the field and the other with that for guiding the telescope (Fig. 13). A knob to move an oblique mirror is operated by hand to select one of them. In the field-view eye-pieces, with 1°05′ field, is inserted a reticle with a lattice-work cuttings of which lengthwise and breadthwise spacings are all 10′.

The guide eye-end is attached by one of such eye-pieces as Kerner 25 mm, Orthoscopic 13 mm, and Orthoscopic 9 mm, which give the field of 20′, 9′, and 6′, respectively. This eye-end is mounted on a double-slide carrier, which can offset the eye-piece by as much as ±31′, namely about ±30 mm on the plate in both directions of right ascension and declination.

A few kinds of the reticle which have a single cross, a double cross, and a cross with a central gap are available. These reticles are not seen directly but the image of them is projected into the field of view. The position angle of the cross can be changed by 90° with an image rotator, and further the reticle can be moved by ± 5 mm with a micro-motor. These devices are prepared for trailing the spectra of stars either in right ascension or declination direction, and for tracking objects which belong to the solar system. The view-field of every eye-piece is furnished with a variable illumination.

A small refractor with 50 mm aperture, 7 magnifications, and 7°16′ field is mounted on each guide telescope near its eye-end. This is used to find out the aiming objects.

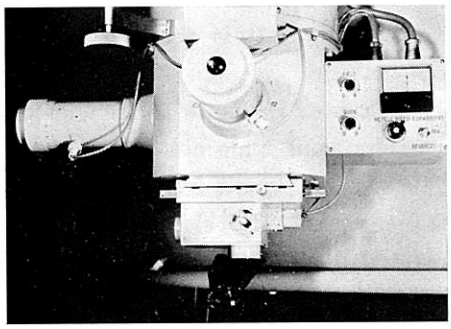

Fig. 13. *The three eye-ends of the guide telescope. Left and upper ones are for viewing the field. Lower one is for guiding the telescope, and is mounted on a double-slide carrier.*

5. Operation and Control of the Telescope

1) The Control System

The telescope is composed of many parts which are not only large and heavy but also furnished with complicated mechanisms, such as a mirror cover, a plateholder carriage, a filter loader, a shutter, a prism rotator, and so on. We can operate these parts as well as the main body of the telescope, easily not by hand but by an electric power. Actually the telescope is equipped with 24 motors, 18 magnetic clutches, and about 70 microswitches.

The control system is indispensable for such a telescope to be operated systematically well as a whole and to fulfil its function satisfactorily. A minicomputer has been introduced to our system

in order to assist us to handle the telescope. It increases the security of the operation which is basically assured by means of the control circuits. A manual operation is, however, given a priority to the computer-controlled one in our system. We can even operate the telescope putting aside the minicomputer and its peripherals, since the values of time, and of position and focus of the telescope are all indicated by circuits independent of the minicomputer, and every handling is possible by pushing buttons manually.

A block diagram of the control system and its relating parts is shown in Fig. 14, (a).

2) The Hardware

The main control system is located in an air-conditioned control room (Fig. 15, (a)). An observer sitting in front of the control desk can look out over the observing floor and the telescope through the window. Electric cables and wires connect each part of the system with the telescope as well as the dome. About 500 wires bundled in 18 cables with excellent flexibility are laid in the polar axis.

The second operation panel and monitor TV are equipped on the observer carrier (Fig. 9, (a)), which is always exposed to the outdoor condition. It has been designed to work well against any low temperature down to -20°C and high humidity up to 100%. It is connected to the equipments located in the control room through a cable which is movable accompanying with the carrier. Signals to be given to the dome are transmitted by means of wires, laid along the rail on which the dome rides, and of electric shoes which are attached to the dome and slide on the wires.

The central processing unit (CPU) is a minicomputer OKITAC-4300C equipped with 12K words of 16 bit core memory. According to the stored program, the CPU accepts interruptions by an observer, watches conditions of the telescope, achieves necessary calculations, and issues control signals. Somewhat detailed descriptions will be given in the next section. The minicomputer has two peripheral input/output devices, namely a paper tape reader (PTR) and an electric typewriter (ET). The PTR has a reading speed of 30,000 characters per minute, and is used for loading the observation program. The ET has a printing speed of 1000 characters per minute, and the same speeds of reading and punching paper tapes by means of its attachment. It is used for printing and punching observation records, and outputs of the encoders *etc.*

The process input/output device (PIO) connects electrically the control system with the telescope and the dome. It accepts signals from microswitches and detectors, and transmits them to the display panel and the CPU. On the other hand, it transmits control signals from the observer and/or the CPU to the telescope and the dome through control circuits. The clock unit is also contained in the PIO, which provides the local sidereal time and the Japan standard time from the built-in oscillator with 10^{-7} accuracy. This unit continues to work even in case of the power failure unless it exceeds three hours.

The control desk is installed with an operation panel, a handset box, a control panel, and a monitor TV. These devices except for the control panel are doubly attached to the observer carrier. The operation panel is furnished with pushbuttons for manual operation of the telescope and the dome, thumb-wheel switches for setting the field number (the sky observable from the site being divided into 1582 fields of $6^{\circ}\times6^{\circ}$ and with their center separated from each other by 5°), and the exposure time, and pushbuttons for interrupting the CPU.

The handset box can be connected either to the telescope tube or the operation panel. It is used for the guide operation, namely, it has change-over and on-off switches of slow and fine motions, a shutter button, and an interruption switch for the guiding job explained later. Being made of ABS plastics, it is light enough to hold and does not benumb a hand of the observer in

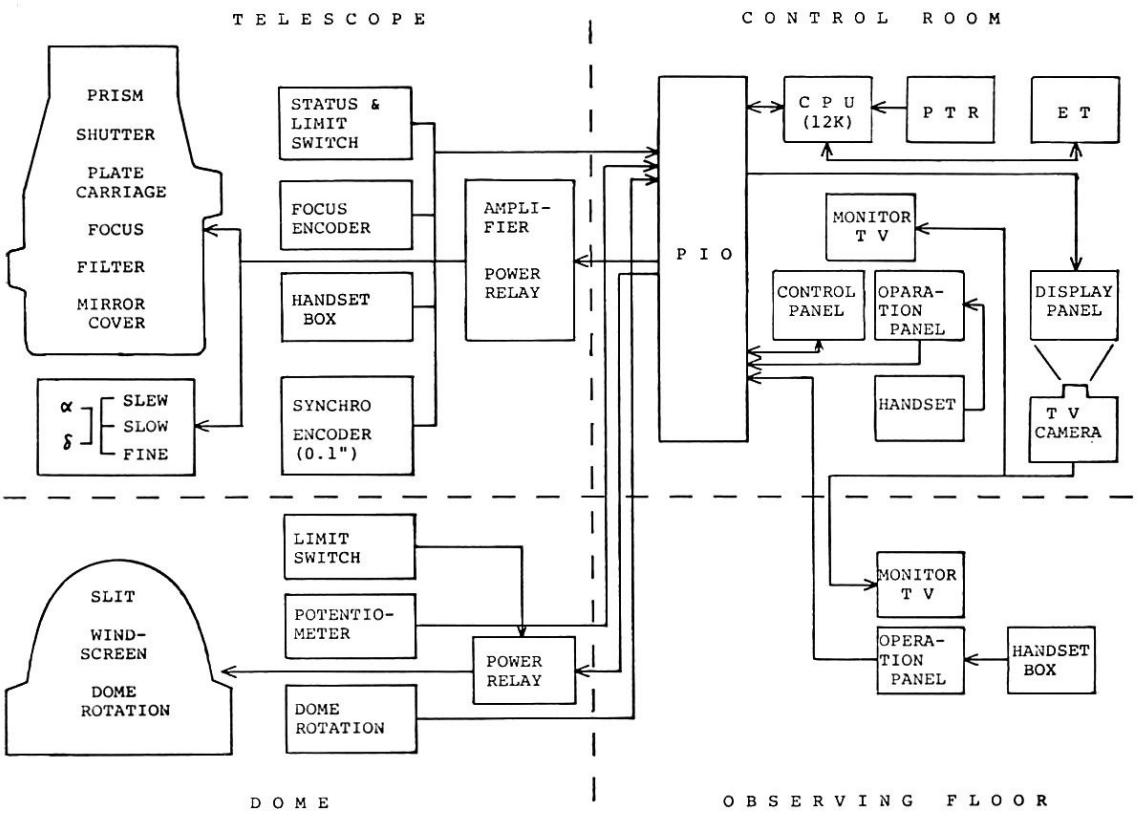

Fig. 14. (a) *A block diagram of the control system and its relating parts.*

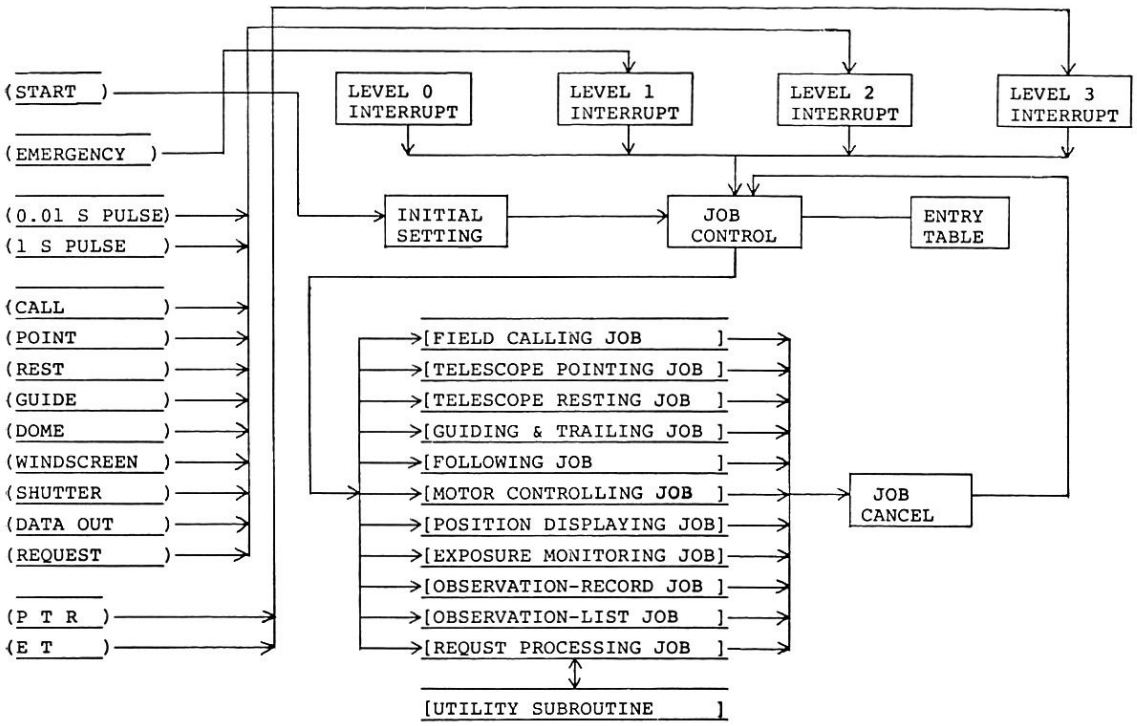

Fig. 14. (b) *A block diagram of the observation program.*

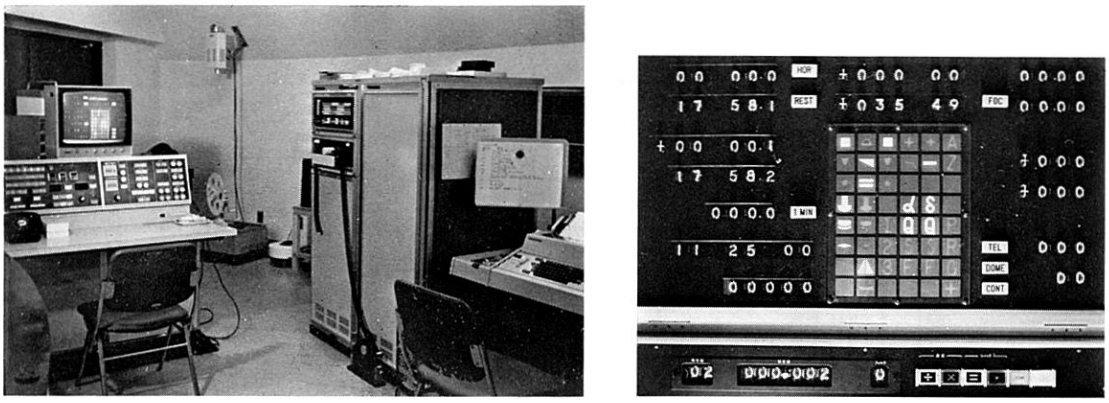

(a) (b)

Fig. 15. *(a) A view of the control room. At the center is located an ensemble of CPU, PTR, and PIO. The control desk seen left side is installed with control panel (left), operation panel (right), and monitor TV (top). ET is at the right side and the display panel and the TV camera are at the farside of the room. (b) A display on the monitor TV. The upper main portion is for telescope and dome, and the lowest line for sky monitor.*

winter.

The control panel is provided with buttons of main power, thumb-wheel switches for setting the time, control switches for supplying dry air and warm air, and dislpay lamps of every kind of limit conditions and warnings. It is mainly used for preparation of the observation and in any emergency occasion.

A display panel is located at a corner of the control room, which is reproduced with monitor TVs at the control desk and the observer carrier by means of a TV camera (Fig. 15, (b)). At the central part of the display panel, several kinds of the symbol marks are illuminated according to the status of each part of the telescope; e. g., opened or closed status of the hoodcap, the shutter, and the mirror cover; on or off status of the secondary mirror, the carriage, and the filter; the driving speed of the telescope, the number of the selected filter, the vertex direction of the objective prism, and so forth. In addition, the status of the observation program is also indicated.

Around the symbol mark zone, digital values are displayed. The displayed items are given in Table 2 with the readout unit and the detector or the source used. Among them, positions of right ascension, declination, the focus, the dome slit and the windscreen are displayed in pairs of actual values provided by the detector and the preset value instructed by the computer.

Since the display panel covers all of the data which are necessary for the observation, the observer can collect a whole information simply by looking into the monitor TV.

3) The Software and the Telescope Operation

An observation program is written with an assembly language. Its block diagram is shown in Fig. 14 (b). The job control corresponds to the main program here, and each job is triggered by a respective interruption. Four levels of the interruption are provided by an internal status of the CPU (level 0), by emergency buttons (level 1), by interruption buttons and time-base pulses of 0.01 second and 1 second (level 2), and by input/output devices, *i. e.*, PTR and ET (level 3), respectively. The priority decreases with increasing level number.

At a time of observation, the program flows as follows: (1) It searches an entry table in the job control, (2) registers a job in the table when an interruption is given, after judging that the condition is satisfied, (3) executes the job, namely, watches, calculates, records, and controls the telescope and the dome, and (4) cancels it in the table and returns to the job control. This program

Table 2. *Items of Digital Displays on the Monitor TV*

Item	Readout unit	Detector or source
Hour angle	0.1 min	Synchro
Right ascension	0.1 min	1)
Declination	1′	Synchro
Focus	0.01 mm	Encoder
Dome slit (Azimuth)	1°	Encoder
Windscreen (Zenith Distance)	1°	Potentiometer
Exposure time	0.1 min	2)
Japan standard time	1 sec	Oscillator
Local sidereal time	0.1 min	Oscillator
Plate number	1	Counter
Increment in right ascension	0″1	Encoder
Increment in declination	0″1	Encoder

1) Local sidereal time minus hour angle.
2) One second pulse of Japan standard time.

in which all jobs are put equally in a row and the job control controls them, has an advantage to make it possible that plural jobs can be processed in parallel.

Now we shall mention each step of a sequence of observation. In the following, Gothic letters mean interruptions given to the CPU.

At first the observer pushes power buttons at the control panel, and loads the observation program from the PTR. Then he starts the program and enters the observation data using the ET; date, observer's name, and objective prism number (if not used the number 0 is given). Besides, he must enter the data of field positions, focus values, and filter names if they are different from the standard ones. (The CPU issues the center position of 1582 standard fields referring to 1950 equinox when their field number is given by thumb-wheel switch on the operation panel). The CPU computes the necessary data which are output by the ET in a printed list format.

The observer now comes to the observing floor with the list in hand. After confirming that the telescope is in normal state by looking into the monitor TV, he moves the telescope tube to the rest position, *i. e.*, the nearly horizontal posture with its top toward north, and takes off the hoodcap. He turns off lights and opens the dome slit. Next he loads a plate into a plateholder in the dark room, mounts it to the carriage from the loading box of the telescope tube, and sends it to the exposure position. Then he gets in the observer carrier.

The observer makes choice of the filter. He **calls** the field to be photographed which is set by means of the thumb-wheel switch. The CPU computes again and displays the center position of the called field (right ascension, declination, azimuth, and zenith distance). It gives warning in case that the telescope cannot reach the field position. The observer inspects the displays, and then **points** the telescope and the dome. The CPU computes corrections to the preset position arising from precession, atmospheric refraction, and deviation due to the objective prism. Thus the CPU drives the quick and/or slow motors of the polar and declination axes and the focus motor to bring the telescope and the plateholder to each preset position. When the dome slit and the windscreen are in **automatic** mode, the CPU also moves them to each preset position. The telescope is controlled to take the shortest course which passes well above the horizon to reach the position.

After this has been finished normally, the observer moves the observer carrier to the eye-end of the guide telescope. He chooses a guiding star, setting it on the cross mark of the reticle.

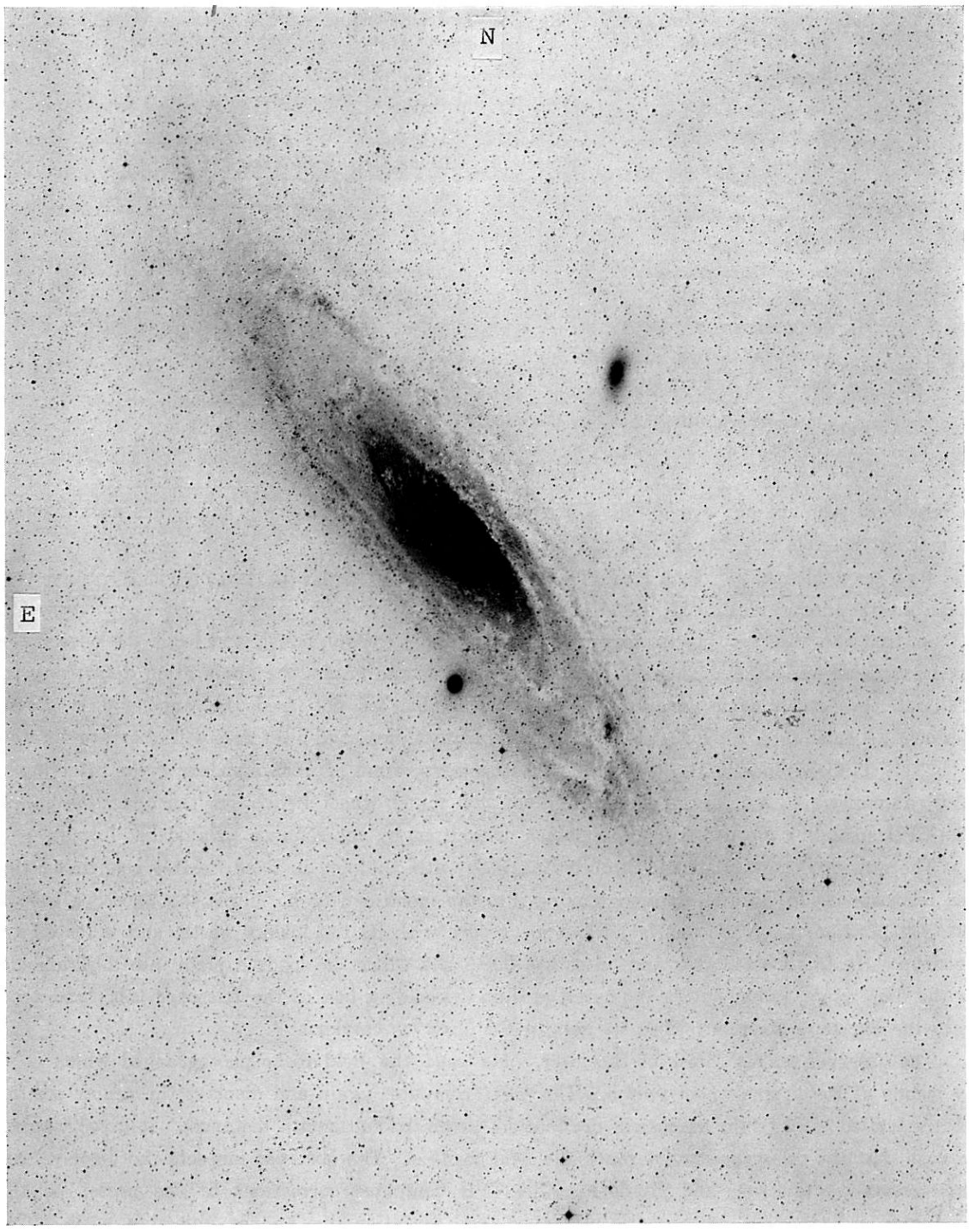

Fig. 16. (a) *M 31 exposed on Eastman Kodak IIaO plate with Schott GG 385 filter for 30 min. (A part of the original scale copy of the Plate No. K 82). An area in the lower right corner region was examined to estimate the limiting magnitude referring to Baade and Swope (1963).*

Fig. 16. (b) *Comet West (1975 n) exposed on IIaO plate with no filter for 10 min. on March 14, 1976 (A part of the original scale copy of the Plate No. K 285).*

He sets the exposure time with the thumb-wheel switch, and opens the mirror cover. Then he **opens** the shutter and guides the telescope by means of the handset box. The CPU memorizes the exposure time and the telescope position, and watches the exposure successively. The CPU drives the dome and the windscreen in accordance with the telescope position.

In the **guiding** mode, the monitoring of the guiding operation is processed by the CPU. It reads the count of 0.1 encoders attached to the both axes and issues the values. These outputs have been used for the analysis of the telescope motion (see 6, 2)). Furthermore in this **guiding** mode, we can let the CPU guide the telescope in some given way if so desired.

The CPU **closes** the shutter when the exposure reaches the preset value. Then it prints and punches the observation record by means of the ET. The observer closes the mirror cover and pushes the **rest** button. The CPU takes the telescope to the rest position, where the observer puts the carriage out, and unloads the plateholder from the telescope. He takes the plate out of the holder in the darkroom, and thus finishes one cycle of the observation.

4) Some Features of the System

Now several features of our control system will be mentioned.

The first one is that it is equipped with highly reliable electric parts which have been produced by ever progressing electric techniques; transistors, ICs, long life pushbuttons, microswitches, relays, and highly flexible cables.

It may be the next feature that most parts of the system are equipped in an air-conditioned control room. This arrangement has been adopted not only because such devices as CPU do not work well in severe circumstances of the observing floor, but also because we are attempting to make it possible that all operations except for the plate loading are accomplished inside the control room by improving the system accompanying with an introduction of the new guiding device.

Merits of the system with the minicomputer and the digital display are summarized as follows.

(1) Security of the telescope operation increases.

(2) Excellent reproducibility of the position makes it easy to intercompare photographic plates.

(3) Highly reliable observation records can be obtained, and good filing system may be easily established.

(4) Flexibility of the control system is large, for different kinds of operations which will hereafter be introduced one after another.

6. Observational Examinations on Performances of the Telescope

1) Optical Performances

(a) The limiting magnitude

We took photographs of three selected sky fields where the magnitude of very faint stars had been accurately determined photoelectrically. The data of the photographs and the references of the fields taken are shown in Table 3.

Table 3. *Data and References for the Determination of the Limiting Magnitude**

Plate Number	Exposure	Background density (ASA Diffuse)	Featured object in the field	References
K 82	30 min	0.56	M 31	Baade and Swope (1963)
K 123	60	0.60	NGC 2403	Tammann and Sandage (1963)
K 569	60	1.04	M 33	Sandage and Johnson (1974)

* All plates are taken on Eastman Kodak IIaO emulsion behind a Schott glass filter GG 385.

Magnitudes of the faintest star on the plates were examined referring to the identification chart and the magnitude table given in the above-listed articles. The B magnitudes of the faintest stars which are barely visible on our plates were determined as 20.51 for K 82, 20.89 for K 123, and 20.91 for K 569. The limiting B magnitude of the telescope is in this way estimated to be fainter than 20.9 mag.

According to Baum (1962) the limiting magnitude m_l is given by

$$m_l = M - 2.5 \log \alpha - 2.5 \log k + 2.5 \log f + 1.25 \log E - 2.5 \log (1+R), \quad (1)$$

where M is the magnitude per steradian of the sky background, α the angular image size on a plate in radian, k the coefficient of certainty, f the focal length of the telescope in cm, E the granulation density of the plate per cm^2, and R the ratio of instrumental background to sky background.

By photoelectric photometry of the sky brightness at the Kiso station it is known that $M=-4.9$ mag/str ($=300S_{10}$); in our cases of the plates K 123 and K 569 the measured image size $\alpha=10^{-5}$ rad ($=2''$), and $f=330$ cm. Adopting the values of $k=5$, $E=10^7$/cm^2, and $R=0$, equation (1) gives $m_l=20.9$ mag which is identical with the value obtained above.

(b) The image size

The image size of stars on several good quality plates was examined by measuring them with a microphotometer (Fig. 33). The half-width of the intensity profiles of their images, for which the correction of the sky background is applied, is nearly constant irrespective of their peak intensity.

We adopted this value of the constant half-width as the image size of the stars on the measured plates. The result is 40–50 μm for the plates which were exposed for 2–10 minutes at the seeing condition of 2–3″.

(c) The Hartmann test

An extensive Hartmann test was carried out with various combinations of emulsions and filters, and in various situations of the telescope. We used the Hartmann disk over which about 260 holes of 2.5 cm diameter are arrayed with uniform lengthwise and breadthwise spacings of 5 cm. This one makes it possible to obtain homogeneous data of the image-forming quality at every point on the corrector plate and the mirror surface. Several pairs of intrafocal and extrafocal Hartmann images (Fig. 17) were measured by a comparator (Fig. 35) and the two-dimensional analysis for the Hartmann constant and the focus value was executed by the minicomputer in the control room.

Calculated values of the Hartmann constant are plotted in Fig. 18 versus the wavelength. As the Hartmann constant T corresponds to the radius of a star image given in arc second, our value of $T=0.76-1.0$ means that the image size due merely to the optical quality of the telescope is 1″.5–2″.0, namely 24–32 μm on a plate. Since the seeing size at the site is usually not smaller than 2″, the image sizes of stars on the skilfully guided plates are estimated to be as much as 40–50 μm, which agree well with the value obtained in the preceding section. The fact that T is minimum at the B color band may reflect that the corrector plate has been figured with 4358 Å as the basic wavelength.

The one-dimensional analysis was further practised both in X and Y directions. The obtained Hartmann constants are $T_x=0.49$ and $T_y=0.43$ at the B band. Fig. 19 is an example of the scatter diagram which shows the distribution of the image point corresponding to each Hartmann hole on the surface of the least confusion. Fig. 20 shows aberration vector diagrams in which the vector of every image point referred to the origin of the scatter diagram is plotted at each position of

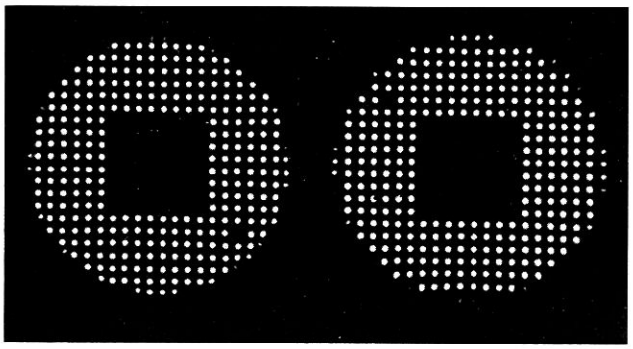

Fig. 17. *A pair of intrafocal (left) and extrafocal (right) images of the Hartmann disk used.*

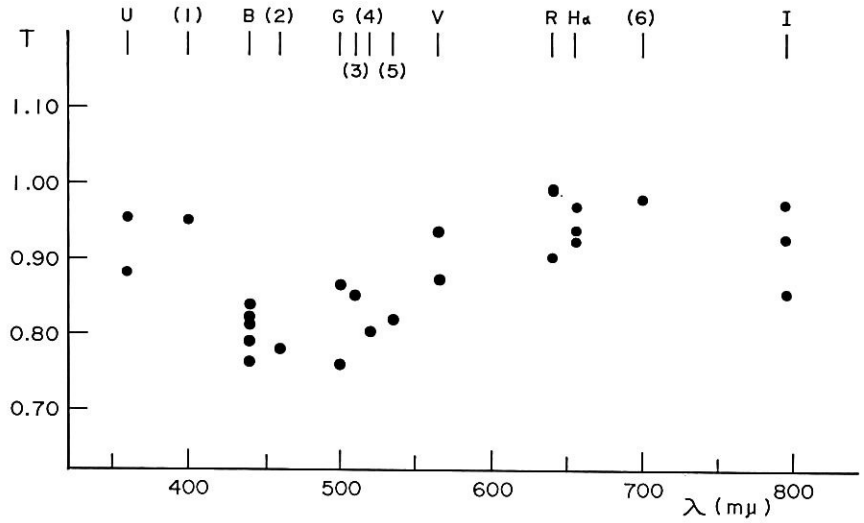

Fig. 18. *Hartmann constants are plotted against the central wavelength corresponding to various color bands shown in Fig.* 12. *Those obtained for special combinations of emulsion (Eastman Kodak) and filter (Schott) are indicated by following key-numerals: (1) 103aO without filter, (2) IIIaJ with GG 385, (3) 103aD with GG 385, (4) 103aF without filter, (5) 103aF with GG 385, and* (6) *103aF with RG 695.*

the corresponding Hartmann hole. These diagrams indicate that there is a slight astigmatism, which seems, however, to matter little. It is apparent from Fig. 20 that the outer part of the corrector plate or the mirror is responsible to some deterioration of the image quality. We learned that when the corrector is rotated, keeping the main mirror and the Hartmann disk fixed, a general pattern of the aberration vector diagram also rotates accordingly. This suggests that the corrector plate is the main cause of the image confusion, though it is by no means serious.

It was further studied whether the Hartmann constant and the aberration vector diagram changed according to various observing positions of the telescope. The test proves that there are little differences among them, the best condition being realized by the position of which hour angle and declination are both 0°. There seems to be little gravitational deformation of the optical system, which apparently affects the image quality. The flexure of the telescope tube is within a tolerable range and the supporting mechanism of the mirror is proved to work well.

The Hartmann test was carried out both in summer and winter to investigate the variation of the focal length with temperature. The result gives the value of 3 μm/deg, which coincides well with the value calculated from the expansion coefficient of the invar bar of 10^{-6}/deg and the focal length of 330 cm. Since the temperature difference at the Kiso station is not more than

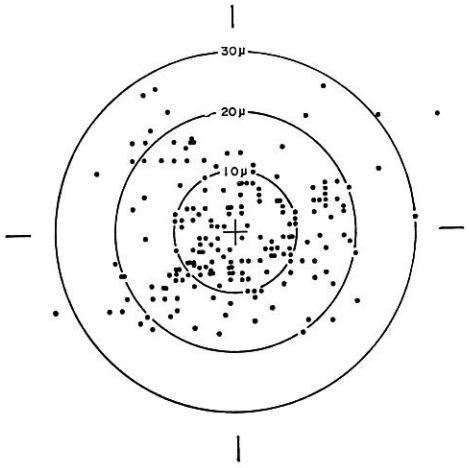

Fig. 19. *A scatter diagram, in the focus, of light rays in B color band from about 250 Hartmann hole areas on the corrector plate and the main mirror. Percentages of light within circles of diameter of 10, 20, 30, and 50 μm (10 μm= 0".625) are 8, 41, 63, and 95%, respectively.*

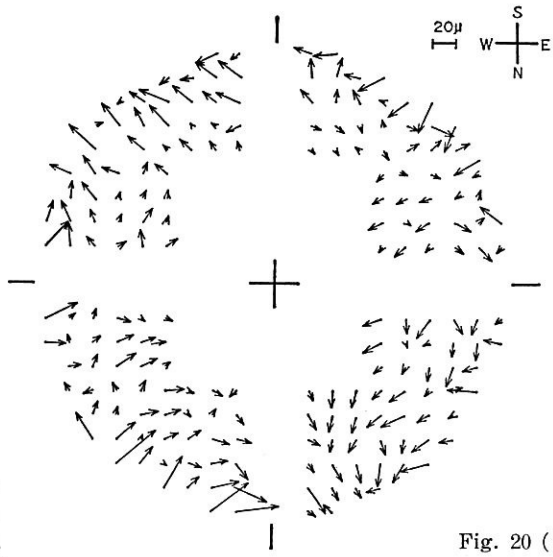

Fig. 20 (a)

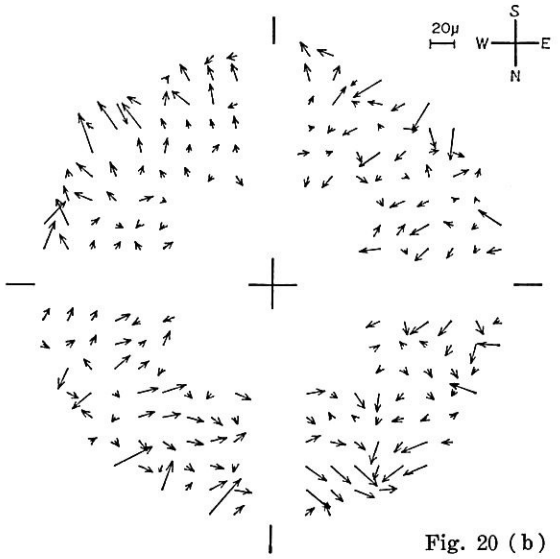

Fig. 20 (b)

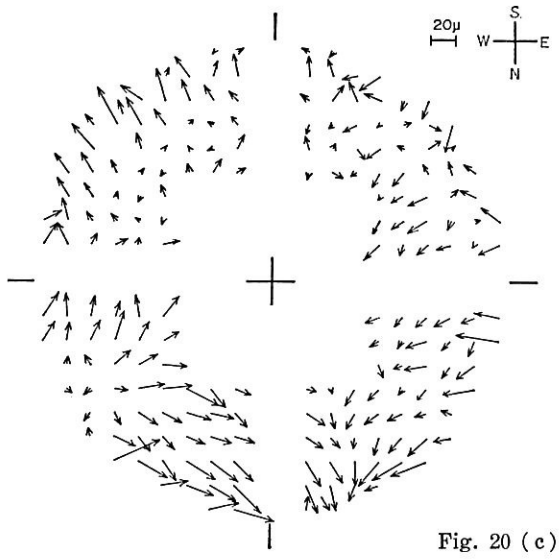

Fig. 20 (c)

Fig. 20. *Aberration vector diagrams of light rays in B color band coming through about 250 Hartmann holes, in the case where the telescope is directed to the sky region of which hour angle H, declination δ, and zenith distance z are respectively, (a) H=−0ʰ5, δ=+30°, z=9°, (b) H=+0ʰ7, δ=−7°, z=63°, and (c) H=−4ʰ8, δ=+24°, z=63°. Hartmann constants obtained for these cases are 0.81 for (a), 0.76 for (b), and 0.94 for (c), respectively.*

30°C, the focal length correction to be applied is at most 100 μm, which is almost the same as the estimated focal tolerance. Therefore it seems not necessary to apply any correction of the focal length due to the temperature difference if the focus is once set at the value corresponding to the mean temperature.

Fig. 21 shows the variation of the focus value as a function of the wavelength, the effects of the differences of the temperature and of the filter thickness being corrected. The focus value at the ultraviolet band differs from that at the infrared band by about 200 μm. The difference due

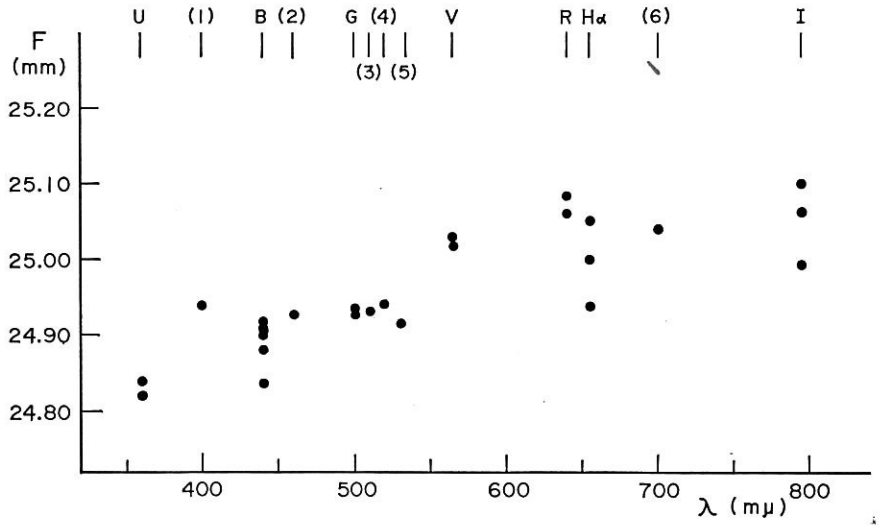

Fig. 21. *The variation of the focus value as a function of the wavelength. The smaller value of F indicates that the focus shifts toward the spherical mirror. Parenthesized numerals mean the same as in Fig. 18.*

to the telescope positions is not appreciable. It is about 50 μm, for example, between two positions where the zenith distances are 0° and 60°, respectively.

Further details of the analysis will be given in Noguchi *et al.* (1977).

(d) Objective prisms

Focus tests of the spectral image were carried out by taking photographs with various focus values of the camera. In case of the No. 2 prism, with a vertex angle of 4°, the position of the best focus for the dispersien direction is distinctly different from that for the trail direction which is perpendicular to the former. To confirm this, a Hartmann test was practised. The Hartmann disk used is the same as that mentioned in the previous section, and the one-dimensional analysis in each direction were processed to determine the Hartmann constant and the difference of the focal length from that in the case where the prism is not equipped. The result is given in Table 4.

The spectral plate is to be taken at the best focus in the dispersion direction, because a trail motion is usually applied in the direction prependicular to it. The 4° prism has also a lens effect which increases the focal length of the camera by considerable amount. On the other hand the 2° prism deteriorates little the original image quality of the telescope.

Dispersion and length of the spectra on the plate are determined by the refractive index of the prism glass which varies as a function of the wavelength as well as by the focal length of the telescope. These are given in Fig. 22.

Table 4. *Hartmann Constant and the Focus Difference When the Objective Prism is Equipped*

Prism (vertex angle)		No. 1 (2°)	No. 2 (4°)
Dispersion direction	Hartmann constant*	0.59	0.70
	Focus difference	+0.12 mm	+1.87 mm
Trail direction	Hartmann constant*	0.62	1.40
	Focus difference	+0.02 mm	+1.02 mm

* These are calculated by one-dimensional analysis from the plate taken in I color band, and are to be compared with T_x and T_y for I color in the case where the prism is not equipped.

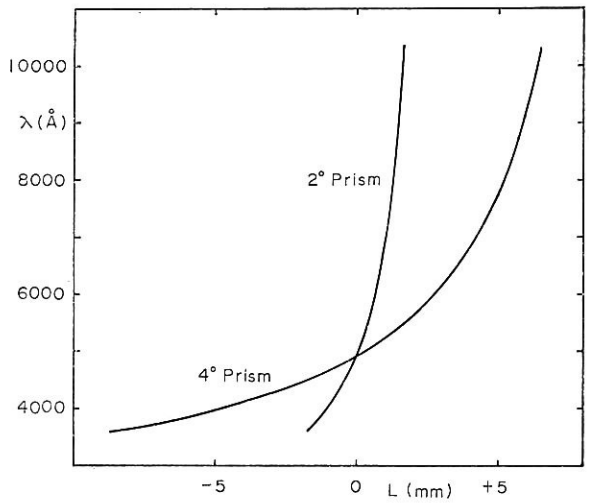

Fig. 22. *Dispersion curves for two objective prisms. Abscissa L indicates the length of the spectra on a plate, and ordinate λ is the wavelength. The origin of L is taken at λ=4861Å.*

Following preliminary results were obtained from observations using these prisms.

The stellar spectra taken with the 2° prism can be classified into several divisions respectively including O-B, late B-A, F-G, K-early M, and late M types. For 4° prism spectra, the classification into intervals of a few subdivisions of each type can be applied, and further the determination of the luminosity class seems possible to a certain degree for spectra with large luminosity effects. S and C type stars can clearly be distinguished from each other and from M type stars by means of molecular bands appearing in wide wavelength regions. The stars of which spectra have conspicuous emission lines, such as Wolf-Rayet, Mira type, and Be stars, can be picked up from the 2° prism photographs; in the 4° prism photographs, however, many lines are well separated and identifiable.

The spectra of nearby spiral galaxies and of nearby galaxies with active nuclei are featured by such emission lines as Balmer and several forbidden lines. Markarian's method to find out fainter active galaxies is also applicable to the spectra obtained by the 2° prism without trailing.

Fig. 23 gives examples of the objective prism spectra. Single trails with two different speeds are consecutively practised on the same plate to extend the magnitude range of stars of which spectra can be precisely measured. In case of the trail with a single speed, this range is about two magnitudes, and in the case where two speed trail is applied, the range can well be doubled. A movable reticle set in the eye-piece of the guide telescope (see 4, 5)) is used for trailing, but not convenient for a non-uniform trail. Computer-controlled non-uniform trail with an appropriate program is now under consideration.

We have used several kinds of emulsions for test observations. Eastman Kodak IIaO and IIIaJ are for shorter wavelength regions and IIaF (or 103aF) and IN are for wider regions. The spectra ranging from 3500Å to 8800Å, taken on IN emulsion with no filter, are most suitable for determining the wavelength dependency of the stellar radiation. Further the A band arising in the red region due to an atmospheric absorption is seen to be fairly sharp in the 4° prism spectra taken on IN emulsion seem to be good references to measure the radial velocity of the stars. In the 2° prism spectra taken on IIaF or IN emulsions, a hump occuring in the green dip has conspicuous appearance and may play the same roll as the A band in the 4° prism spectra.

2) Mechanical Performances

(a) Analysis of the telescope motion

As mentioned in section 5, 3) the correction given to the telescope motion by the guide

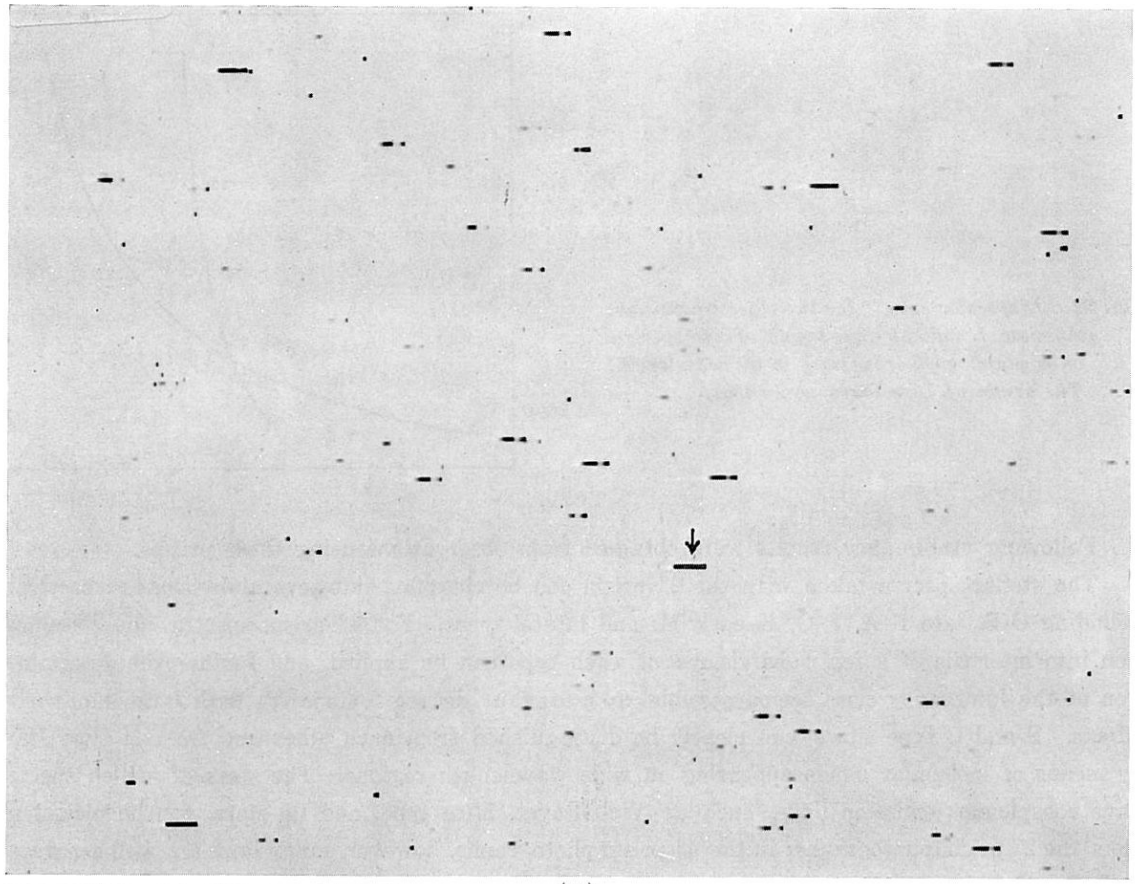

(a)

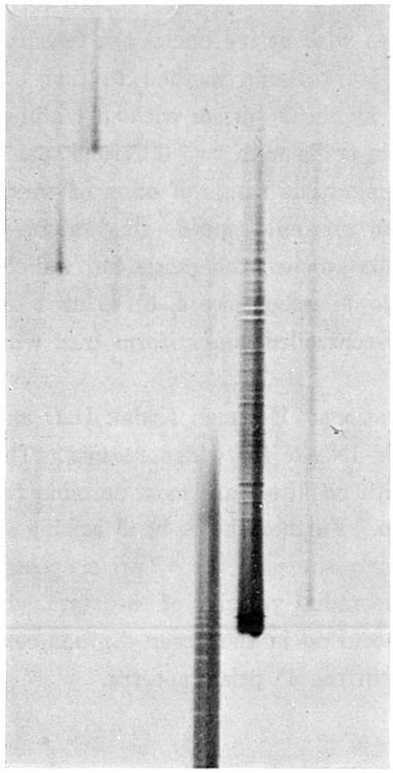

(b)

Fig. 23. Examples of the objective prism spectra. For all plates North is top and East is at the left.

(a) Original scale copy of 2° prism spectra taken on Eastman Kodak IN emulsion without filter for 10 min (Plate No. K 395). An arrow indicates P Cyg.

(b) Enlarged copy of the 4° prism spectra taken on 103aF plate without filter for 7.7 min on Oct. 27, 1976 (Plate No. K 557). The star which shows the spectrum with conspicuous emission lines is Nova Vulpeculae 1976. Trailing speed is 1″/sec, but for the first 1.7 min 20 intermittent trails of 1 sec duration per every 5 sec, and for remaining 6 min 12 trails of the same duration per every 30 sec were carried out.

(c) and (d) A pair of the original scale and enlarged copy of the 4° prism spectra taken on IN emulsion without filter for 32.5 min. The photographed area is a part of Perseus region (Plate No. K 470). Trailing speed and the duration of each intermittent trail is the same as in the case (b), with two sets of 30 trails, for the first 2.5 min at every 5 sec, and for following 30 min at every 1 min. In (d) the spectral type and the photographic magnitude of these stars seen in upper, middle, and lower parts respectively are F8 (7.8 mag), B3 (5.6 mag), and G5 (7.8 mag) according to AGK3 Catalog. The absorption line appearing near the left end (longer wavelength side) of each spectrum is the A band.

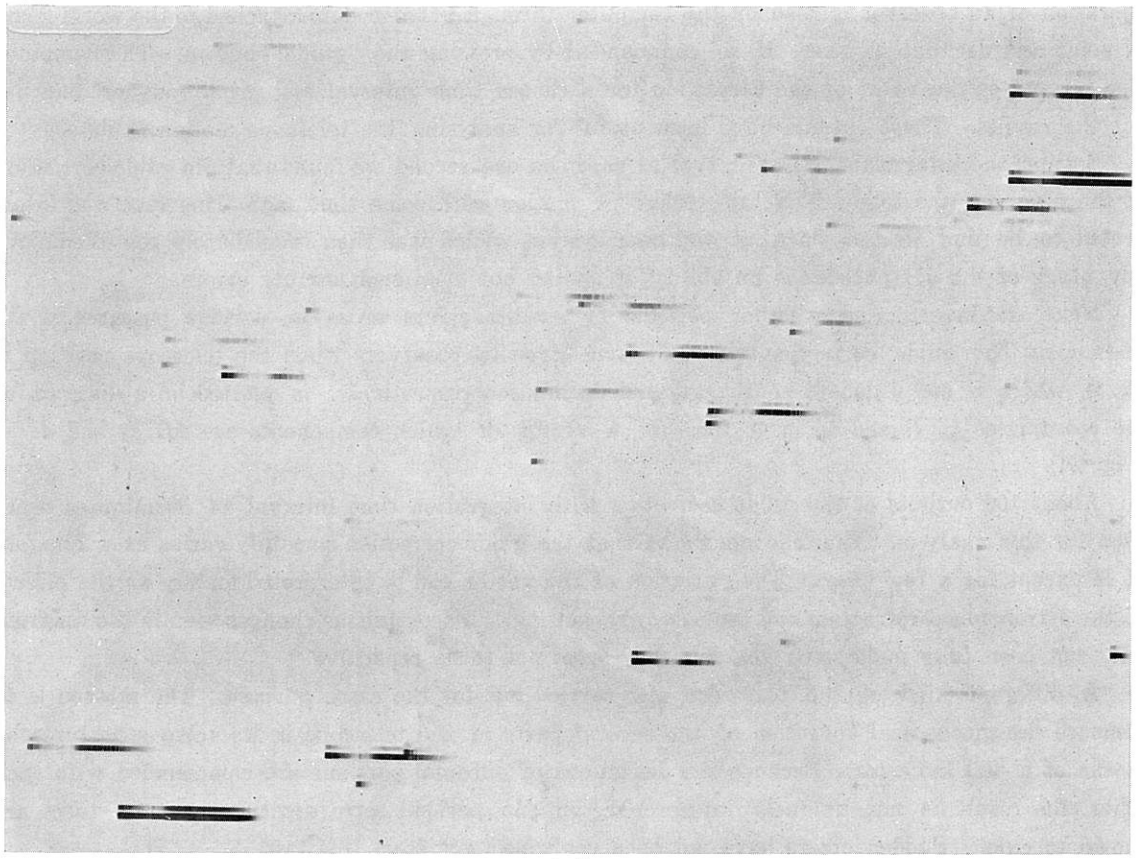

(c)

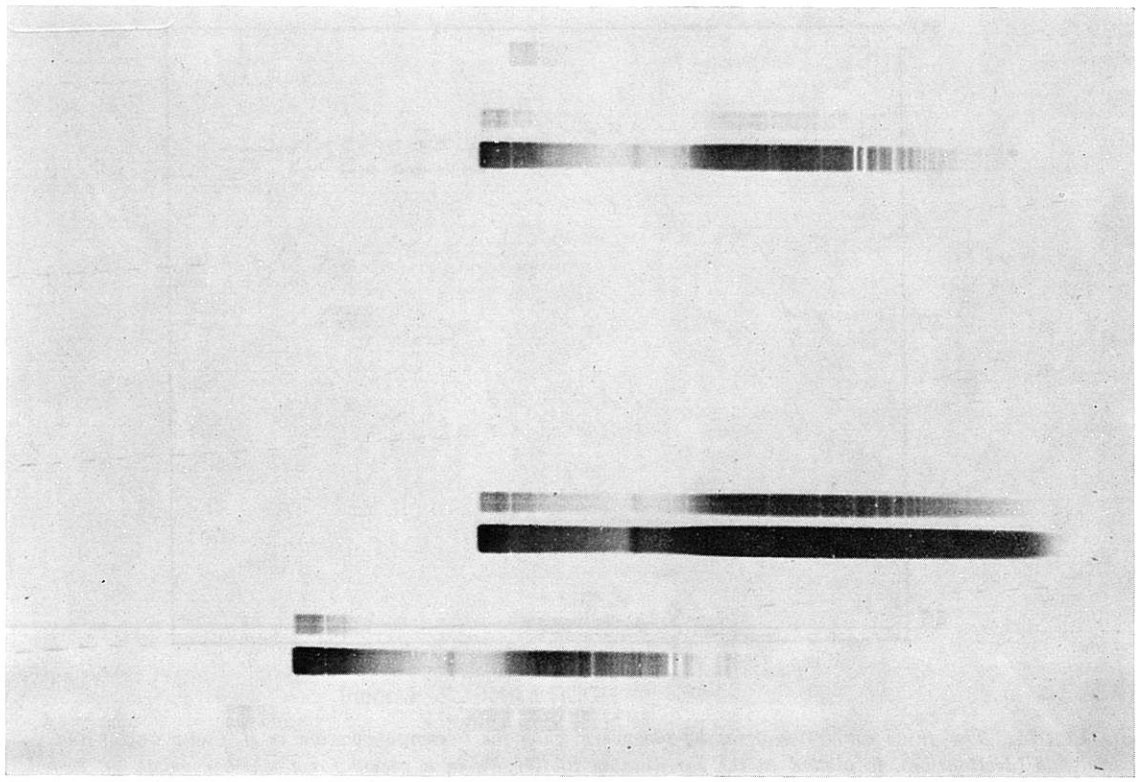

(d)

operation of an observer is read by the computer through 0".1 encoders attached to the worm gears of polar and declination axes, if so commanded by pressing the "guide" button. The computer also integrates the value of the correction for a chosen time interval and prints out or punches out the results. These outputs have been useful for analysing the telescope motion in detail.

Setting the integration time interval as short as one second we found that the guide correction of the observer was followed by the telescope motion with some time lag. This fact was interpreted to be due to the slack of the gear system, which was then immediately remedied. An advantage of the 0".1 encoder is an ability of finding out even such minute errors.

Next we investigated whether periodic or sudden errors arose in various postures of the telescope. The guide correction per unit time given by observers when the telescope position is (H, δ), where H and δ denote hour angle and declination respectively, is plotted on a diagram at the coordinates of H and δ, in a form of a vector of which components are dH/dt and $d\delta/dt$ (Fig. 24).

About 100 outputs of the guide correction with integration time interval of 30 minutes were used for this analysis. The diagram shows that the guide correction smoothly varies as a function of H except for a few cases. The variation of the vector can be interpreted mainly as the effects of the astronomical refraction and the polar axis setting. Discontinuous changes seen in the diagram have not been fully understood yet, but they seem not to be repetitive.

A different kind of the test was also carried out for the same purpose. The method is to measure the mechanical deflection of the several parts of the telescope in its various postures by means of a dial indicator. Because the deflections of different portions are compounded with each other, the result is not uniquely interpreted, but no periodic errors with varying postures are shown to exist. Sudden errors have not been confirmed yet from this test.

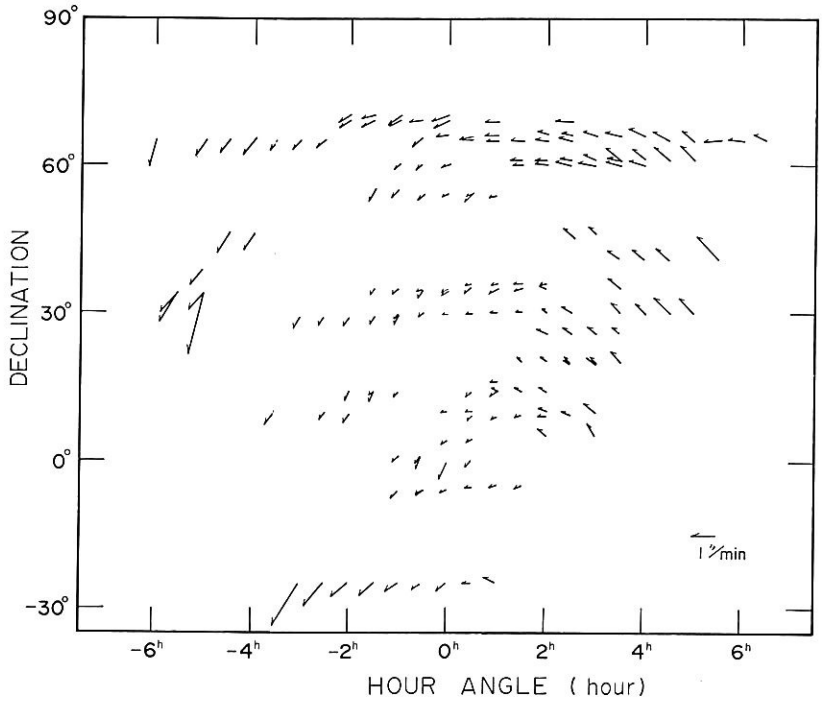

Fig. 24. *The guide correction given by observers when the telescope position is H (hour angle) and δ (declination), is plotted at the coordinates of (H, δ), in a vector form which consists of two components dH/dt and dδ/dt.*

(b) The setting of the polar axis

On a large field plate taken by the Schmidt telescope, it is usually seen that star images in its outer region stretch more or less. The longer the exposure time the larger the stretch. This is due to the differential refraction which depends not only on the zenith distance of the sky field but also on the direction of the polar axis. As recently long time exposures for deep sky survey and for special color band observation have become increasingly important, it seems worth trying to reduce this effect as far as possible.

First we tried to recognize the actual direction of the polar axis in the following way which was a modification of the method used by Shimizu (1963). Its principle is shown in Fig. 25. Let us choose a circumpolar star A which is very near to the pole. It rotates around the true pole T, but both A and T are subject to nearly the same refraction, so A is apparently observed to go around the refracted pole R, and it moves to B during the time interval of Δt. If the polar axis of the telescope is directed to P which is near but different from R, the observer will see that the declination of the star, δ, changes by $\Delta\delta = \mathrm{PA} - \mathrm{PB}$ during Δt, $\Delta\delta$ being a function of hour angle of the star, which shall be designated by H. Further denoting the distance between P and R by a, and the hour angle of P referred to R by h, Shimizu (1963) obtained the following formula for the case where a is very small;

$$d\delta/dt = -a \sin(H-h). \tag{2}$$

We can similarly derive its counterpart of the right ascension as

$$d\alpha/dt = -a \tan\delta \cos(H-h). \tag{3}$$

The record of the 0.″1 encoder provides us accurate values of $d\delta/dt$ and $d\alpha/dt$. Fig. 26 shows the values thus obtained of $d\delta/dt$ and $d\alpha/dt \cot\delta$ plotted against H for each star. Then a and h and accordingly the position P are determined from each of equations (2) and (3) by means of the least squares method. Full line curves in Fig. 26 show sine and cosine curves drawn with thus obtained a and h. These curves fit to the observed data well, but the positions of P derived

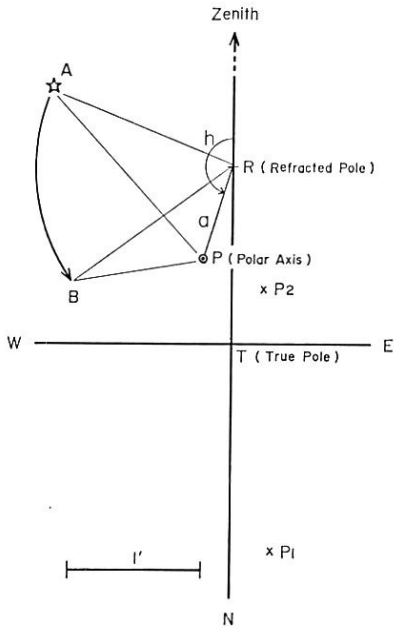

Fig. 25. *Geometry for obtaining the telescope pole from the motion of a circumpolar star which is very near to the celestial pole. P_1 and P_2 are the telescope positions as determined by equations* (2) *and* (3), *respectively.*

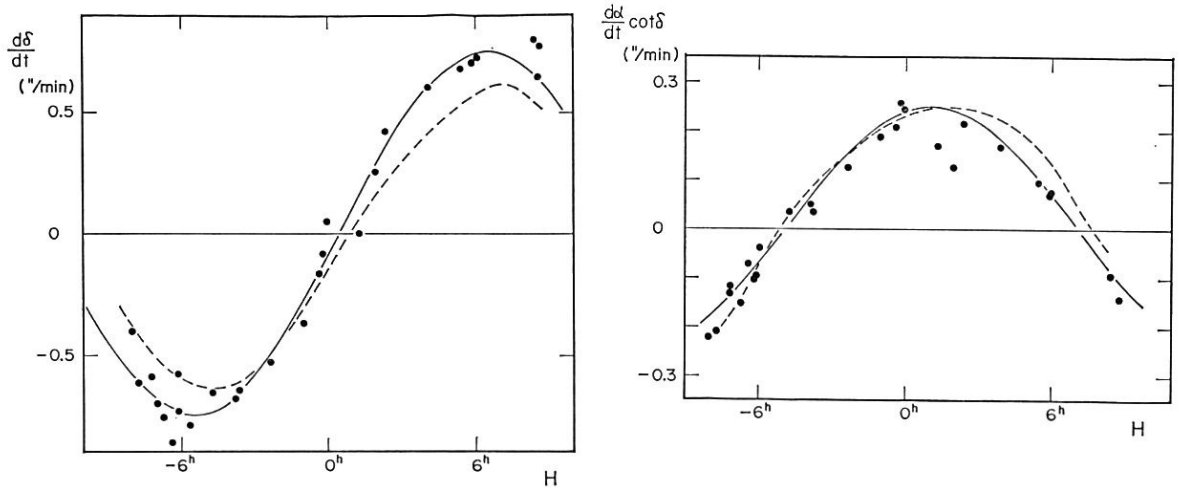

(a) (b)

Fig. 26. *Values of the guide correction plotted against hour angle of the star.*
(a) Declination component and (b) Right ascension component.

from equations (2) and (3), P_1 and P_2 respectively, are different from each other by about 2′ as shown in Fig. 25.

Embarrassed by this result, we tried to ascribe this inconsistency to the effect of flexure of the telescope. It is conceivable that, for example, the fork arm deflects by an amount varying with hour angle of the telescope, and in this case an effective polar axis will wander about the sky.

To examine this we took photographs of the polar region, rotating the telescope around the polar axis while being exposed. The loci of the star image on the plate are not circular but slightly distorted, probably owing to the flexure. From this distortion we estimated the variation of the flexure as a function of hour angle.

Assuming that the dependency of flexure on hour angle is symmetrical with respect to the meridian, the solution is uniquely obtained. Fig. 27 shows thus derived positions of the effective polar axis corresponding to several hour angles. If the diurnal motion of the stars are doubly photographed on the same plate, with the telescope being fixed for some time interval, the refracted pole R is determined. Thus obtained R and the true pole T which is 81″ north of R at our site, are also represented in Fig. 27.

Under an assumption that there exists really the wandering of the telescope axis as shown in Fig. 27, we can calculate the guide corrections necessary to cancel it. Broken-line curves in Fig. 26 indicate these values in δ and α at each H. Agreement with the observation is generally good, and thus the inconsistency occurring with an assumption of the rigid axis now seems to disappear.

As mentioned above (3, 1)) this flexure is considered to be due to the deflection of the fork arms which amounts as much as 1′. It now becomes clear that its effect on the telescope direction differs at most by 1′ (Fig. 27) depending on the hour angle, namely, on the posture or the relative position of the two arms of the fork.

Next we investigated the influence of the differential refraction on star images in the outer part of the plate, taking into account the wandering of the polar axis. Stretches of the star images due to the differential refraction were calculated for various time intervals and for several

sky regions with different hour angle and declination, by varying the position of the polar axis at its hour angle of 0^h, Q, as a parameter. The optimum position of Q which affords the minimum mean stretch for the i-th sky region, Q_i, was thus obtained, then a mean of these Q_is was derived by giving to each Q_i the weight proportional to its relative frequency of being photographed. This weighted mean optimum position to which the telescope pole is to be set is shown in Fig. 27 as $\bar{Q}$. It is noted that $\bar{Q}$ is located not between the true and refracted poles but rather below the former. Further details of this analysis will be discussed by Hamajima *et al.* (1977).

The polar axis of the telescope was finally set at $\bar{Q}=50''$ below the true pole according to this result. It has been confirmed that this setting gives the least stretches of star images by comparing them with those obtained from other settings which were practised in a sequence of trials. Further calculations prove that the effect of the differential refraction in our case is comparable with that in case of the rigid polar axis which has no wandering with hour angle.

(c) Direction of the guide telescope relative to the main telescope

In the preceeding section we were concerned with the star images in the outer part of the plate. Now let us examine those in the central part.

The image quality of the star with which an observer guides the telescope is affected not only by the observer's skill but also by the stability of the relative direction between the guide and main telescopes. In the case where either or both of them are poor, the star images are subject to distortion even in the central part of the plate. Investigating the quality of these images on about 200 plates all of which are exposed for more than 30 minutes, we recognized that it depends on the telescope posture. Although the distortion of these star images is of the order of at most 1.3 times its diameter, we tried the following test to study whether the parallelism of the guide and main telescopes related to the telescope posture.

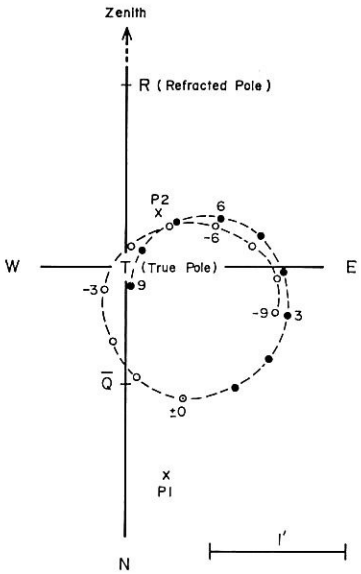

Fig. 27. *The wandering of the telescope pole according to the change of its hour angle which is shown by the numeral in hour. P_1 and P_2 are the same as in Fig. 25, and $\bar{Q}$ is the determined mean optimum direction to which the telescope pole at hour angle of 0^h is to be set.*

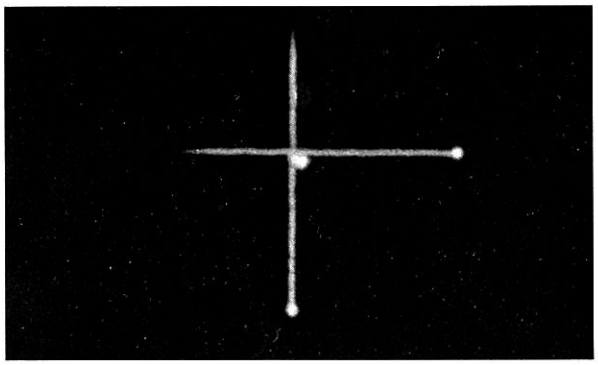

Fig. 28. *A photograph for examining the stability of the relative direction of the guide and main telescopes. Three sky regions are photographed of which hour angle H are 0^h, -4^h, and $+4^h$, respectively, the declination δ being kept constant as $+35°$. The image of a star of $H=+4^h$ deviates from those of other stars.*

First we expose a plate for the zenith region centering a star on a reticle of the eye-piece, and then repeat the exposures for other sky regions centering different stars on the reticle. An example of the test plate is shown in Fig. 28 in which an image of a zenith region star is at the intersection of the cross of two trails, while that of a star of which hour angle $H=-4^h$ and declination $\delta=+35°$, is also very close to the cross point, but that of another star whose $H=+4^h$ and $\delta=+35°$, deviates from it by about 10″.

All of these images should be on the same point if the relative direction between the guide and main telescopes is kept constant during the repeated exposures. This is proved not to be fulfilled when we observe the sky region far west from the zenith.

We examined the displacement of the plateholder supporter, which might take place when the posture of the telescope tube largely changes, with a dial indicator and found that it was less than 10 μm for any posture difference. On the other hand we found that the deviation of the image point seemed a little different for each of the two guide telescopes. These facts suggest that either or both of the guide telescopes are responsible to the image deviation.

Consequently the displacements of objective lens and reticle were examined carefully but no definite evidence for these was found to exist. Although the question thus has not yet been answered, there is no problem practically in usual cases where the plate is exposed for the sky region of which zenith distance is not so extremely large.

7. Accessories of the Telescope and the Measuring Instruments

1) The Sky Monitor

The sky monitor is a digital microphotometer to monitor continuously the sky brightness in the region photographed and in the wavelength range used. It consists of a photometer attached to the telescope tube (Fig. 29), two identical operation boxes each of which is mounted near the eye-end of the guide telescopes, and a display panel located in the control room. This display panel is put aside that of the main control system and is together reproduced with two monitor TVs at the control desk and the observer carrier (Fig. 14, (d)). It contains digital displays of the instantaneous count sampled at every 6 seconds, integrated count after the opening of the exposure shutter, and the filter number, besides several symbol marks which indicate the on/off status of power source, high voltage, and photometer shutter.

The 80 mm objective lens is projected on a R 374 photomultiplier (Hamamatsu TV Co. Ltd., Japan) by a Fabry lens through a ten-position wheel containing various color filters. A square diaphragm to define the sky area and neutral density filters to adjust the sky brightness can also be inserted. To compensate the dark current of the photomultiplier, a chopper wheel is placed in the optical path and synchronized by 125 Hz to up/down counters giving an automatic dark subtraction. It is necessary to estimate the contribution of stars in the photographed area to the sky count if we want to expose a plate to the sky darkness predetermined. The effect of bright stars is corrected individually and that of faint stars by the value depending on the galactic coordinates of the area.

2) The Equipment for Supplying the Dry Air

The dry clean air is produced by the equipment located in the basement of the building and sent up into the telescope tube (Fig. 30). The capacity of the equipment is 60 l/min. The air is compressed to run through a carbon filter, a hygroscopic tube, a gas filter, and a cooling pipe. The pipe line reaches the telescope tube through the polar axis, the west arm of the fork, and the declination axis. The air is blown onto the surface of the main mirror and both sides of the

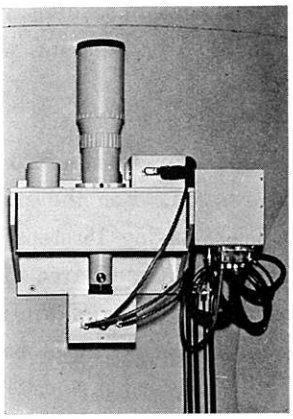

Fig. 29. *The photometer of the sky monitor which is mounted on the telescope tube.*

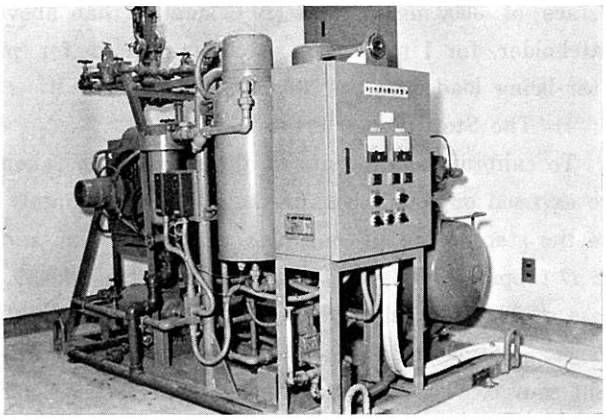

Fig. 30. *The equipment for supplying the dry air.*

corrector plate. A heater is attached to the top portion of the conical tube for warming the air which is poured onto the outer surface of the corrector plate to prevent it from misting or frosting.

3) The Apparatus for Loading a Plate and for the Test Bending

We use either 14 inch or 24 cm square glass plate of 1 mm thick. It should be kept bent to form a spherical surface of 3300 mm radius during the exposure. For this purpose we use the apparatus shown in Fig. 31 (a), when we load a plate into the plateholder. A backside lid of thick metal with the spherical surface on one side and 8 hooks on the other side is pressed onto the plate uniformly, and then the hooks are turned for locking the lid firmly to the holder frame.

Six plateholders for the 14 inch square plates and another six for the 24 cm plates are ready for use. The deviations from the spherical surface were measured at various points over the plates bent by this loading apparatus by means of a dial indicator, and it was found that they were at most ± 0.05 mm for the 14 inch plates and ± 0.03 mm for the 24 cm plates which were well within the focal tolerance of the optical system.

The test bending apparatus (Fig. 31 (b)) is further prepared to bend the plate to the curved

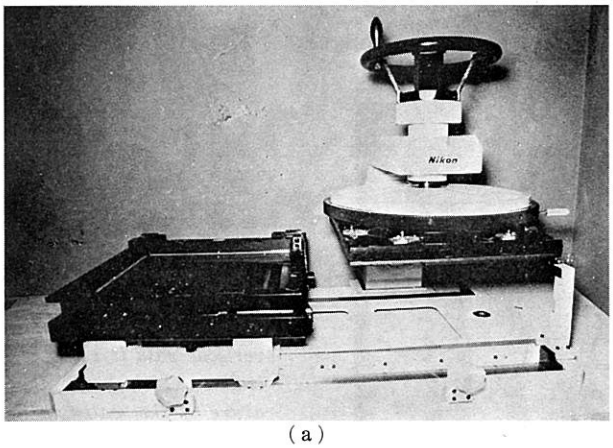

(a)

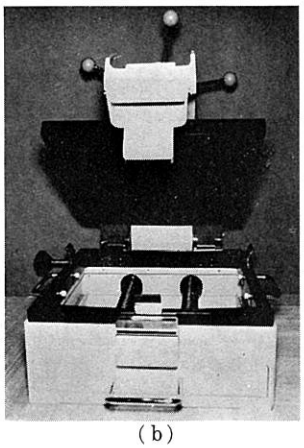

(b)

Fig. 31. *(a) The apparatus for loading a plate into the plateholder. A backside lid is presently detached from the holder. After a plate is inserted, the holder is moved to the position right under the loader and then the lid is pressed down onto the plate, and the hooks are turned for locking the lid.*

(b) The apparatus for the test bending. A plate is inserted in the frame seen lower side, and then the thick metal presser with a curved surface forces the plate to be bent, for 1 minute or so.

surface of 3000 mm radius (10% smaller than above-mentioned radius), before loading it to the plateholder, for 1 minute or so. This is used for preventing the plate from breaking while and after being loaded to the holder.

4) The Step Wedge Printer

To calibrate the density of the photograph taken by the telescope four series of step wedge are exposed on four edges of the plate, immediately after each observation. For the present we use the step wedge of our own making, 20 mm wide and 120 mm long, having 15 steps of every 0.2 D (approximately) and a range of about 3.0 D. The light source is a small area of ground glass which is illuminated by a standard filament bulb and is placed at a distance of 3 m from the wedge. Various color filters and neutral density filters of 5 cm square are set right behind the light source. The exposure time is controlled by a timer.

5) The Equipment for Developing the Plate

A method of nitrogen-burst agitation is adopted for processing the photographed plate (Fig. 32). Five vertical vats are held side by side in a temperature-controlled water bath, each of which contains water for prewashing, developer, short stopper, the first fixer, and the second fixer, respectively. Two or three plates to be developed are inserted in a frame which is vertically soaked into these vats one after another. The five vats are furnished with bubbles which burst up from the bottom into the spaces of 5 mm thick between the plates in the frame. We set the distributor to control the burst duration to be 1 second and the burst interval 10 seconds. The thickness of the space between plates is designed to be smaller than the diameter of bubbles to enable them to strip the exhausted developer off from the emulsion surface and to prevent them from being compounded with each other. The bubble-burst is given by 0.5 atmospheric pressure. These data have been reached by a series of experimental developments which were carried out in a transparent plastic vat. Microphotometer tracing of the step wedge exposed on four edges of many plates shows no detectable nonuniformity.

6) The Microphotometer

In Fig. 33 an automated balance type microphotometer (left) with an attachment for digital output data (right) is shown. Its carriage table is 50 cm square in size and is moved by as much as 23 cm in two rectangular coordinates, so that all the place on 14 inch square plate can be measured. Measuring and reference light beams are alternatively obtained by means of a chopper wheel. The former is defined by four knife-edges set rectangular. The latter passes through a

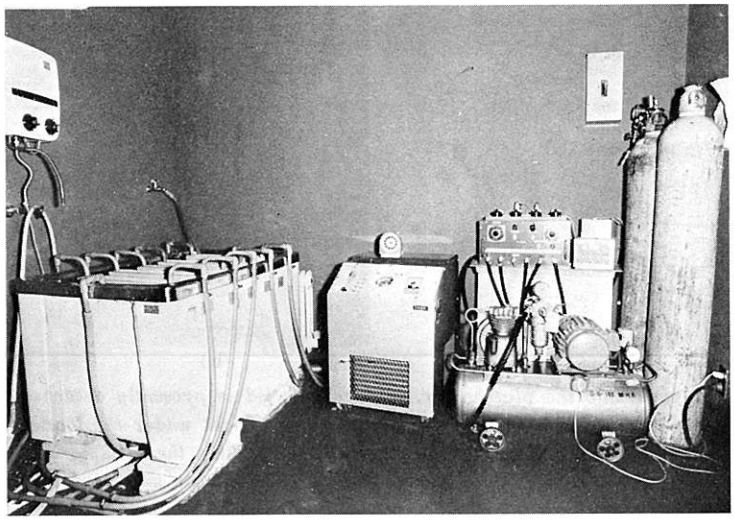

Fig. 32. *An array of the equipment for processing the photographed plate. A bath containing five vertical vats is seen left, a controller which keeps the temperature of the water in the bath to be constant is at the center, and the air-compresser, the distributor, and the nitrogen-cylinders are located right.*

mechanically variable diaphragm which consists of two slits of logarithmic spiral form intersecting each other and rotated in opposite sense by a servomotor. This servomotor is driven by the voltage difference between the generating output of photomultiplier due to the measuring beam and that due to the reference beam. The plate density is read out by an absolute rotary encoder attached to the axis of the servomotor. The sample rate of data is changeable between 1–200 μm in x-axis, and the sampling time can be set differently down to 24 milliseconds. The pitch interval of the raster scan in y-axis is selected as one of 0.05, 0.1, 0.2, and 0.4 mm. The data are recorded on 8 bit paper tapes. The detailed description on this instrument appears in Ishida, Maehara, and Ohashi (1974).

7) The Irisphotometer

The mechanical part of the irisphotometer is featured by a triangle-shaped rigid base frame shown in Fig. 34 (a), which has been designed to enable the large and heavy carriage to move smoothly while preventing it from bending. A frame holding a plate hangs on the carriage which again hangs on the base frame by means of a pulley with a counterweight.

The optical system is also of automated balance type with measuring and reference light beams. The light source is contained in a housing located at the top of the instrument to avoid the effect of the heat. The diameter of the iris diaphragm is read by an absolute rotary encoder attached to it and its value is kept in an up/down counter by a peak-hold circuit. On the other hand the position of the star image is read by incremental linear encoders of 1 μm step in x- and y-coordinates.

The operation panel and the view screen are seen in Fig. 34 (b). The view field and the iris diaphragm are observed with 10 and 30 magnifications respectively on the screen of 15 cm square.

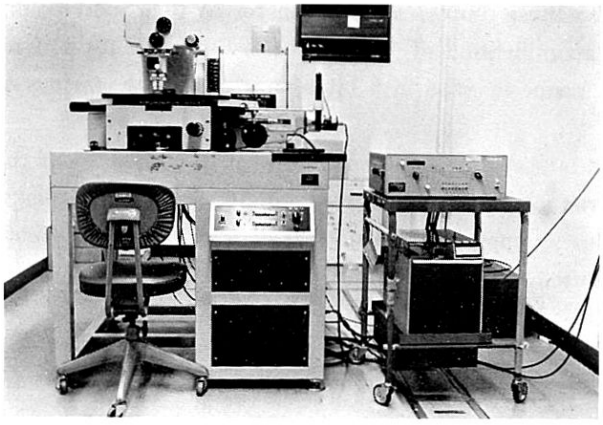

Fig. 33. *The microphotometer. Main body (left) and the attachment for the digital output (right).*

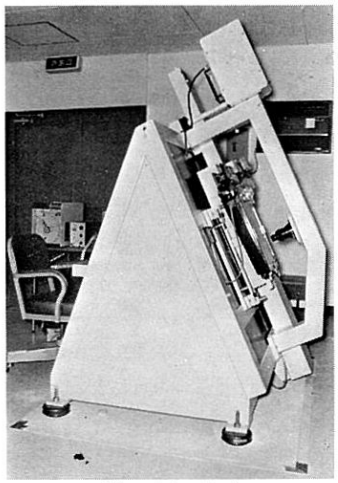

Fig. 34. (a)

Fig. 34. (b)

Fig. 34. *The irisphotometer. Its main body (a) and operation panel (b).*

The data are punched on 8 bit paper tapes. An output paper tape can be used as an input tape. The preset is performed with 0.1 mm accuracy in both coordinates, by driving motors with two alternative speeds of 10 and 1 mm/sec. A full description will be given in Ishida, Maehara, and Ohashi (1977).

8) The Blink Comparator

The mechanical part of the blink comparator is similar to but still larger than that of the irisphotometer, for it has to carry on two plates to be blinked (Fig. 35). The position of the left plate is adjustable by as much as ± 5 mm in x- and y-directions and the right plate can be rotated by up to $\pm 2^\circ$ so that both plates are projected identically on a view screen.

Two plates are projected alternatively on the screen of 15 cm square, with a blinking frequency of 1, 2, 5, or 10 Hz. We can select 7 or 35 magnifications, the former of which gives the view field of about 20 mm square and the latter 4 mm square area of the plate, respectively.

The operation panel is analogous to that of the irisphotometer. The ways in which the position of star images is read out and the data are recorded and preset, are also the same as those for the irisphotometer. Moreover the format of the punching paper tape is common and exchangeable between the two measuring instruments. For details see Ishida, Maehara, and Ohashi (1977).

9) The Isophotometer

The isophotometer has been designed to employ a one-dimensional array of 500 photo-diodes (CCD 101, Fairchild, U.S.A.) as a detector for the purpose of high speed raster scanning.

The mechanical structure is alike that of the irisphotometer (Fig. 36). The light source is an electric bulb of 650VA, which is controlled to keep the brightness constant by means of a servomechanism. It illuminates the plate area of 50 mm square uniformly. The detector is a charge coupled device with contiguous sensitive area of 30 μm square each, its total length being 15 mm. The image to be measured is projected onto these diodes, which transfer in turn individually and consecutively their electric charges. The magnification of the projector lens is either 1 or 1/3. Their electric charges are recorded on a magnetic tape in 8 bit binary code with various speeds up to 10 kHz.

The sensitivity of the individual diodes is stable in time and shown fairly a good linear relation to the light intensity within the dynamic range of a little larger than 100. We approximate the sensitivity characteristic of individual diodes by appropriate equations of which constant coefficients are determined in each measuring run, and used for the correction. A further numerical treatment

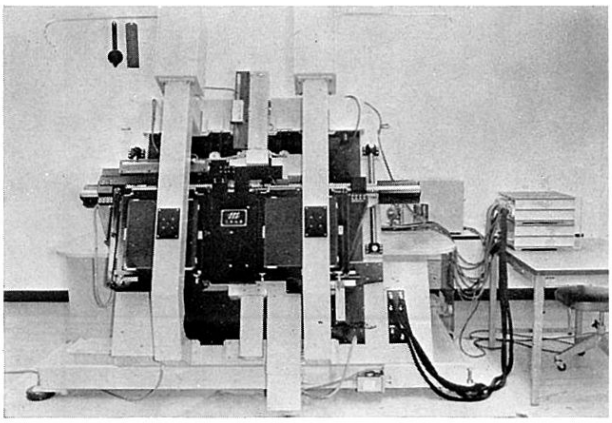

Fig. 35. *The blink comparator. Two plates to be blinked are seen hanging on the carriage.*

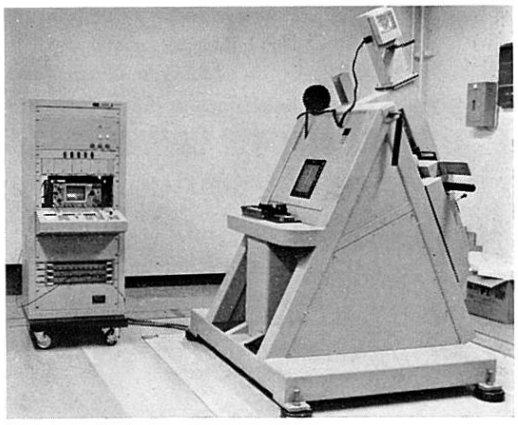

Fig. 36. *The isophotometer. Its main body (right) and the control unit (left).*

is performed by a large computer. Details are given in Maehara and Ishida (1977).

Acknowledgement

The authors would like to thank Messrs. T. Aoki, T. Soyano, W. Tanaka and A. Miyashita for their assistance in carrying out the test observations and reductions, and in preparing drawings and photographs; and Dr. Y. Yamashita for his comments on examinations of the telescope.

References

Baade, W. and Swope, H. H. 1963, *Astron. J.* **68**, 435.
Baum, W. A. 1962, *Astronomical Techniques*, vol. 2 of *Stars and Stellar Systems* (Chicago, The Univ. of Chicago Press), p. 1.
Hamajima, K., Takase, B., Shimizu, M., Aoki, T. and Soyano, T. 1977, *Tokyo Astronomical Observatory Report* (in Japanese), to be published.
Ishida, K., Maehara, H., and Ohashi, M. 1974, *ibid*, **17**, 70.
Ishida, K., Maehara, H., and Ohashi, M. 1977, *ibid*, to be published.
Maehara, H. and Ishida, K. 1977, *ibid*, to be published.
Noguchi, T., Ishida, K., Shimizu, M., Noguchi, T., Aoki, T. and Soyano, T. 1977, *ibid*, to be published.
Sandage, A. and Johnson, H. L. 1974, *Astrophys. J.* **191**, 63.
Shimizu, M. 1963, *Tokyo Astronomical Observatory Report* (in Japanese), **13**, 211.
Tammann, G. A. and Sandage, A. 1968, *Astrophys. J.* **151**, 825.